

Structure and age of volcanic fissures on Mount Morning: A new constraint on Neogene to contemporary stress in the West Antarctic Rift, southern Victoria Land, Antarctica

Timothy S. Paulsen[†]

Department of Geology, University of Wisconsin Oshkosh, 800 Algoma Boulevard, Oshkosh, Wisconsin 54901, USA

Terry J. Wilson[†]

Byrd Polar Research Center and School of Earth Sciences, The Ohio State University, 108 Scott Hall, 1090 Carmack Road, Columbus, Ohio 43210, USA

ABSTRACT

Antarctica is characterized by a unique combination of active processes, including active crustal deformation, volcanism, and glacial loading and unloading, but little is known about the Neogene to contemporary geodynamic state of the Antarctic plate. This paper presents new data on the structure and timing of volcanism on the Mount Morning shield volcano, with the purpose of defining Pleistocene stress directions concomitant with volcanism and rifting in the southern portion of the Victoria Land rift basin. Elongate vents and vent alignments indicate parasitic volcanism has predominantly occurred along a primary set of NE fissures. Parasitic basaltic cinder cones yield ^{40}Ar - ^{39}Ar cooling ages, presented herein, that range from essentially zero to ca. 3.5 Ma, though mostly of Pleistocene age. The systematic NE trend of the fissures on Mount Morning records magmatically induced fracturing of the volcano flanks controlled by a regional N31°E maximum horizontal stress (S_h) that dominated the Mount Morning area during the Pleistocene and, probably, also the Pliocene. Minor volcanism occurred along shorter NW alignments that have no discernible age difference from the NE fissures. The Pleistocene age of the parasitic volcanism suggests that the stress direction documented at Mount Morning represents the contemporary differential stress field in the area. This NE S_h direction differs from the N15°W S_h direction measured in a borehole at Cape Roberts, 100 km to the north, and the S_h orientations

appear to track the changing trend of the segmented rift boundary. The exact cause for the variability in the S_h directions is uncertain, but the change in S_h could record different stress provinces within the rift system, or it could reflect stress reorientation along the major lithospheric boundary of the rift. The new contemporary stress datum at Mount Morning is consistent with a neotectonic normal-fault to strike-slip fault regime within the Terror Rift, which was active in Pliocene-Pleistocene times and could remain active today. This stress regime still dominates the contemporary geodynamic state of this sector of the West Antarctic Rift system.

INTRODUCTION

The West Antarctic Rift system (Fig. 1A) represents one of the largest continental rifts on Earth (LeMasurier, 1990), and it is marked by the large-magnitude Transantarctic Mountain uplift (Stern and ten Brink, 1989; Bott and Stern, 1992; ten Brink et al., 1997), neotectonic faulting (Davey and Brancolini, 1995; Jones, 1997; Salvini et al., 1997), and widespread active or young volcanism (LeMasurier, 1990), yet little is known about the Neogene geodynamic evolution of the rift and rift-flank uplift system. An understanding of the Neogene to contemporary stress field of Antarctica is important because it has fundamental implications for models of Antarctic intraplate stress and deformation (Johnston, 1987; Bott and Stern, 1992; Coblenz et al., 1995; Rossetti et al., 2000; Wilson, 1995), glacial loading and unloading (Wu and Johnston, 2000; Stewart et al., 2000; Ivins et al., 2003), volcanism (Kyle and Cole, 1974; Kyle, 1990b; Rocchi et al., 2002, 2003; Finn et al., 2005), and plate-driving forces (Zoback, 1992;

Steinberger et al., 2001; Lithgow-Bertelloni and Guynn, 2004). Globally, most stress data are derived from earthquake and drilling data (Sperner et al., 2003). In Antarctica, the nature of the Neogene to contemporary stress field is largely unknown because seismic events of sufficient magnitude for focal mechanism solutions have not been recorded (Reading, 2002, 2006), and there has been little drilling. Volcanic vent alignments have long been established as an important source of stress data from continental regions (Nakamura, 1977; Nakamura et al., 1977; Suter, 1991; Bosworth et al., 1992; Suter et al., 1992; Zoback, 1992; Bosworth and Strecker, 1997; Chorowicz et al., 1997; Korme et al., 1997; Adiyaman et al., 1998), yet modern vent alignment studies have not previously been carried out on Antarctica's widespread volcanic fields to constrain the nature of the Neogene to contemporary stress field within the West Antarctic Rift system (Fig. 1A).

This paper presents structural and geochronological analyses of elongate vents and vent alignments on the Mount Morning shield volcano in the southern portion of the Victoria Land rift basin adjacent to the Transantarctic Mountain rift flank (Figs. 1A and 1B). Mount Morning is one of the most suitable polygenetic volcanoes in Antarctica for conducting a paleostress analysis based on fissure orientations because the main shield edifice is Pliocene to Pleistocene in age, relatively uneroded, and has an extensive field of parasitic vents related to fissure eruptions on its flanks (Wright-Grassham, 1987; Wright and Kyle, 1990a). Until this study, isotopic dating and mapping of the parasitic vents on Mount Morning were still at a reconnaissance level. The results presented herein provide a significant advance in our understanding of the spatial and temporal patterns of volcanism in

[†]E-mails: paulsen@uwosh.edu; wilson.43@osu.edu.

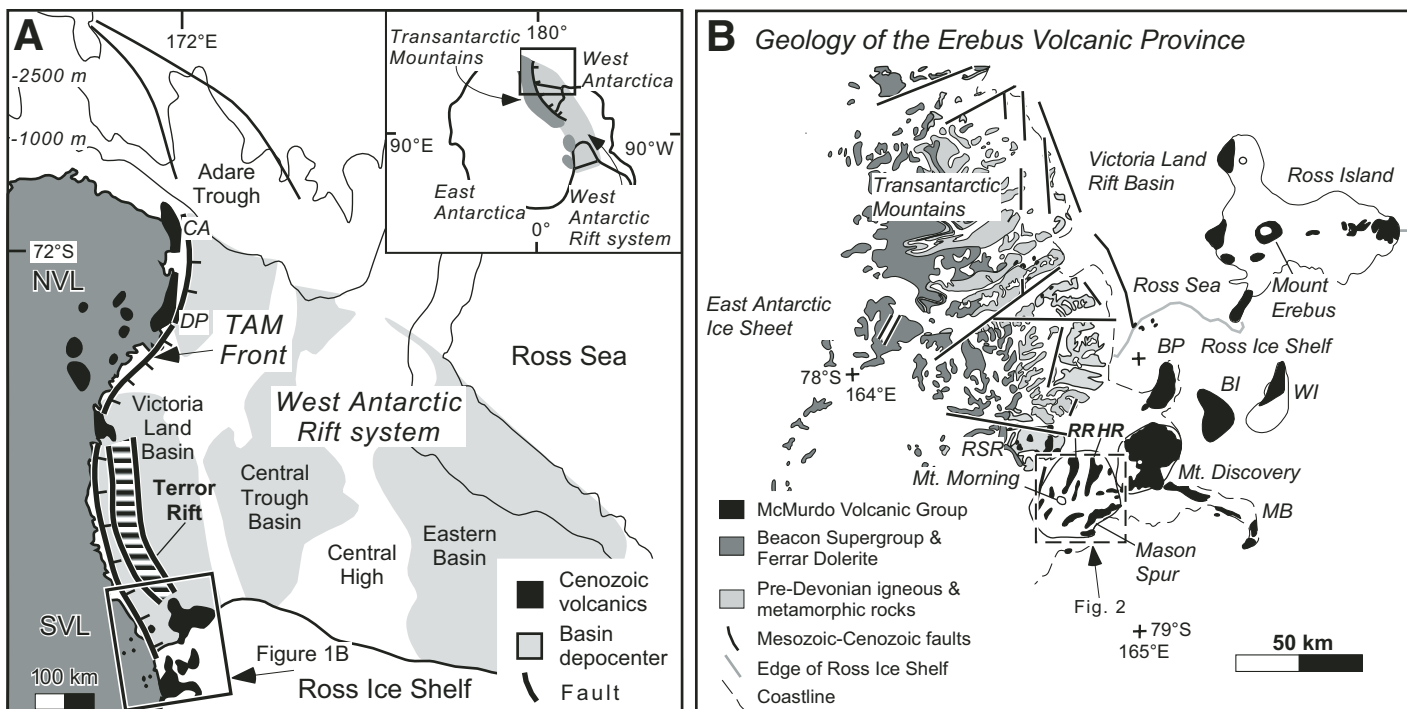


Figure 1. (A) Ross Sea rift basins (pale gray shade) and Transantarctic Mountains (TAM) rift-flank uplift (dark gray shade) are components of the West Antarctic Rift system. Volcanic rocks of the McMurdo Volcanic Group (Cenozoic volcanic rocks shown in black) have intruded and erupted in association with rifting. Aeromagnetic surveys suggest the presence of volcanic rocks in submarine portions of the West Antarctic Rift system in the Ross Sea (not shown). Western Ross Sea rifting is inferred to link with oceanic spreading in the Adare Trough. NVL—northern Victoria Land, SVL—southern Victoria Land. Box shows the location of the Erebus Volcanic Province shown in B, the focus of this study. (B) Geologic map showing Mount Morning and other volcanoes and volcanic outcrops of the Erebus Volcanic Province in the western Ross Sea region (compiled from Warren, 1969; Wilson, 1995). Box shows the location of Figure 2, the focus of this study. BI—Black Island; BP—Brown Peninsula; CA—Cape Adare; DP—Daniell Peninsula; HR—Hurricane Ridge; MB—Minna Bluff; RR—Riviera Ridge; RSR—Royal Society Range; WI—White Island.

the West Antarctic Rift system, serve to constrain the direction of the stress field concomitant with Pliocene to Pleistocene volcanism on Mount Morning, and provide new insight into the greater issue of the Neogene to contemporary Antarctic intraplate stress field. Throughout this paper, we use the 2004 International Commission on Stratigraphy time scale definition of the Neogene Period and Pleistocene Epoch as extending from 24 Ma and 1.8 Ma to the present, respectively (Gradstein et al., 2004).

GEOLOGIC BACKGROUND

Mount Morning is an elongate, ~30-km-wide, 36-km-long, Neogene polygenetic shield volcano located in the Erebus Volcanic Province, which is part of an extensive alkali volcanic province represented by the McMurdo Volcanic Group in the western Ross Sea sector of the West Antarctic Rift system (Figs. 1A and 1B) (Bosum et al., 1989; Kyle, 1990a, 1990b; Behrendt et al., 1991, 1996; Damaske et al., 1994). The summit of the volcano reaches 2723 m

above mean sea level and is marked by a NW elongate caldera with long and short axes of ~4.9 km and 4.1 km lengths, (axial ratio of long axis/short axis = 1.2; Wright-Grassham, 1987; Paulsen and Wilson, 2007). Ice and snow nearly completely cover the southern flank of the volcano. On the northern, northeastern, and southeastern flanks of the volcano, an extensive field of parasitic vents produced by fissure eruptions occurs on Riviera Ridge, Hurricane Ridge, and Mason Spur (Figs. 2 and 3) (Wright-Grassham, 1987; Wright and Kyle, 1990a, 1990b). The parasitic vents (mainly cinder cones and endogenous domes) are phonolitic (upper slopes) and basaltic (lower slopes) in composition (Fig. 2) (Wright-Grassham, 1987; Wright and Kyle, 1990a), and they unconformably overlie Miocene (18.7–11.46 Ma) basalts and trachytes (Wright-Grassham, 1987; Kyle and Muncy, 1989; Wright and Kyle, 1990a, 1990b). Wright and Kyle (1990a) referred to the Miocene volcanic rocks as a subvolcanic complex in the sense that they are highly eroded and unconformably overlain by much younger volcanic

rocks that are associated with the main growth of the shield volcano. These Miocene rocks rest unconformably on early Paleozoic Koettlitz Group basement rocks (Fig. 2) (Muncy, 1979; Wright-Grassham, 1987; Kyle and Muncy, 1989; Wright and Kyle, 1990a). This study focuses on the shapes and alignments of the young parasitic cones and domes on the shield volcano slopes built above the Miocene volcanic complex (Figs. 4 and 5).

VENT SHAPE, ALIGNMENT, AND AGE ANALYSES

Approach to Study

We applied Nakamura's (1977) technique to determine the Pliocene to Pleistocene paleostress direction in the Mount Morning area using the orientation of fissures on the flanks of the volcano. Volcanic fissures typically develop due to magmatically induced hydraulic fracturing of the flanks of a volcano. Flank fissures initiate as fractures near the central conduit of a volcano

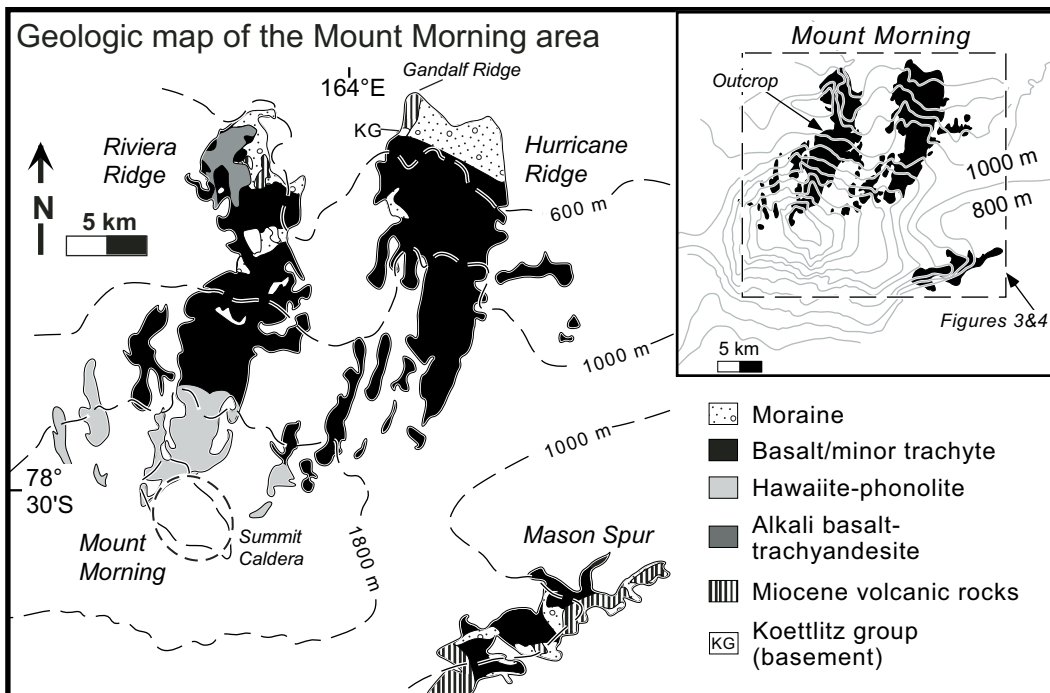


Figure 2. Geologic map showing the principal rock types on the Mount Morning shield volcano (modified from Wright-Grassham, 1987; Wright and Kyle, 1990a). Exposures of volcanic rocks occur to the N, NE, and E of Mount Morning's summit caldera. Miocene volcanic rocks unconformably overlie Paleozoic basement rocks at the northern tips of Riviera and Hurricane Ridges. Pliocene to Pleistocene volcanic rocks, which are associated with the growth of the shield volcano, unconformably overlie eroded Miocene volcanic rocks. Basaltic rocks dominate the lower volcano slopes, whereas phonolitic rocks dominate the upper slopes. Parasitic vents (not shown) occur throughout these areas and were mapped in this study. Box shows the location of Figure 3, the focus of this study.

and then propagate outward in the direction of the regional maximum horizontal stress (S_h), in some cases on opposite sides of the volcano (MacDonald, 1972; Nakamura, 1977, and references therein). Fissures commonly develop concomitant with summit eruptions, presumably because of increases in hydrostatic pressure associated with a rising magma column within the central conduit of a volcano. Hydrostatic pressures increase until they reach the sum of the tensile strength of the surrounding rock and the least external compressional stress, at which time a tensile hydrofracture (i.e., an instantaneous strain release) forms in an orientation that is perpendicular to the least horizontal stress (S_h) and parallel to the S_h direction (e.g., Anderson, 1951; Haimson, 1975; Nakamura, 1977). Magma intrudes these tensile fractures at depth, forming feeder dikes, which in turn fuel eruptions at surface vents aligned along the subsurface trace of the dike (Figs. 6A–6C) (Nakamura, 1977; Nakamura et al., 1977). On a regional scale, the feeder dikes and overlying vent alignments will radiate in all directions for the first few kilometers from the summit caldera because

the hydrostatic stress state of the magma within the central conduit of the volcano dominates the regional stress field. Beyond these distances, hydraulic fractures will systematically curve to assume relatively straight traces that are parallel to the regional S_h direction (Fig. 6B) (Odé, 1957; Muller and Pollard, 1977; Nakamura, 1977; Nakamura et al., 1977). If volcanism occurs within a regional stress field characterized by a differential state of stress, repeated hydraulic fracturing and fissure eruptions over the lifetime of the volcano results in swarms of vent alignments with systematic orientations, which can be integrated with age data to provide temporally constrained fissure and crustal stress patterns (Nakamura, 1977).

Fissure eruptions commonly initiate as continuous “curtains of fire,” but differential cooling causes eruptions to become localized at several points (MacDonald, 1972; Delaney and Pollard, 1982), producing alignments of circular or elongate vents (e.g., cones, domes, necks) depending on whether the eruptive conduits are pipe or planar shaped (MacDonald, 1972). In many cases, especially on the flanks of polyge-

netic volcanoes like Mount Morning, overlying volcanic flows and pyroclastic material obscure the location of fissures, requiring examination of vent shapes and alignments to determine the location and orientation of underlying fissures. The location and orientation of individual fissures can be determined by mapping: (1) linear ridges (i.e., fissure ridges) composed of lava and agglutinate (e.g., Figs. 6C and 7A), (2) cleft cones, which have cleft-shaped craters rimmed by elongate ridges of pyroclastic rocks (Figs. 6C, 7B, 7C, 8, and 9), (3) elongate cones (Figs. 6C, 7D, and 9), (4) elongate domes, and (5) linear arrays of closely spaced circular cones. The elongation direction of these vents will trend parallel to the strike of the elongate eruptive conduit, which in turn trends parallel to the overall trace of the fissure and subsurface dike (Breed, 1964; Nakamura, 1977; Tibaldi, 1995; Korme et al., 1997). Regional fissures, defined by local fissures aligned with circular and elongate vents, can range from tens of meters to tens of kilometers in length (Fig. 6C) (MacDonald, 1972; Nakamura, 1977; Nakamura et al., 1977; Delaney and Pollard, 1982).

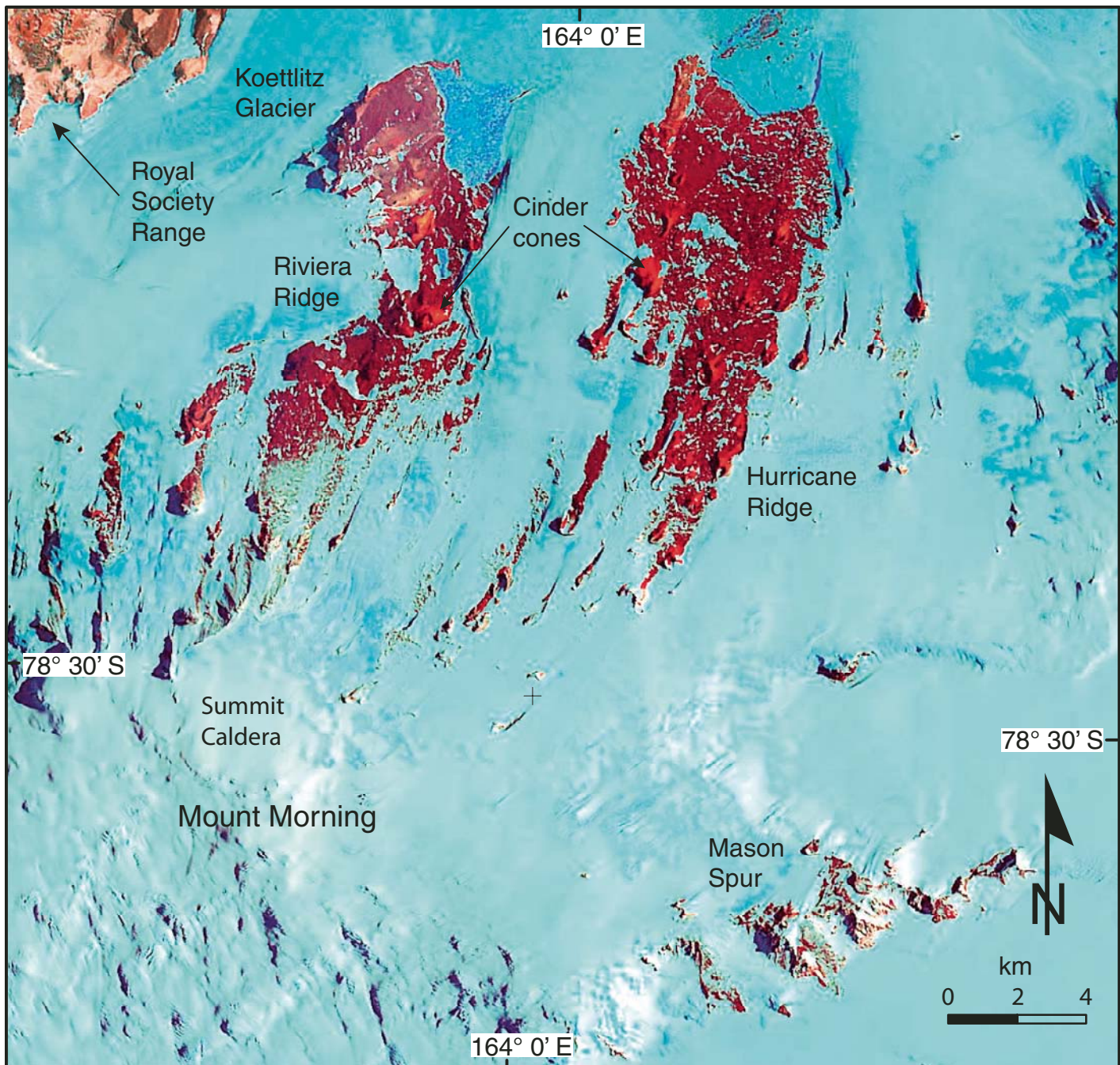


Figure 3. LANDSAT image showing the extensive exposures of volcanic rocks on the Mount Morning shield volcano on Riviera and Hurricane Ridges, as well as on Mason Spur. Ice covers the south-facing slopes of Mount Morning. See Figure 2 for image location.

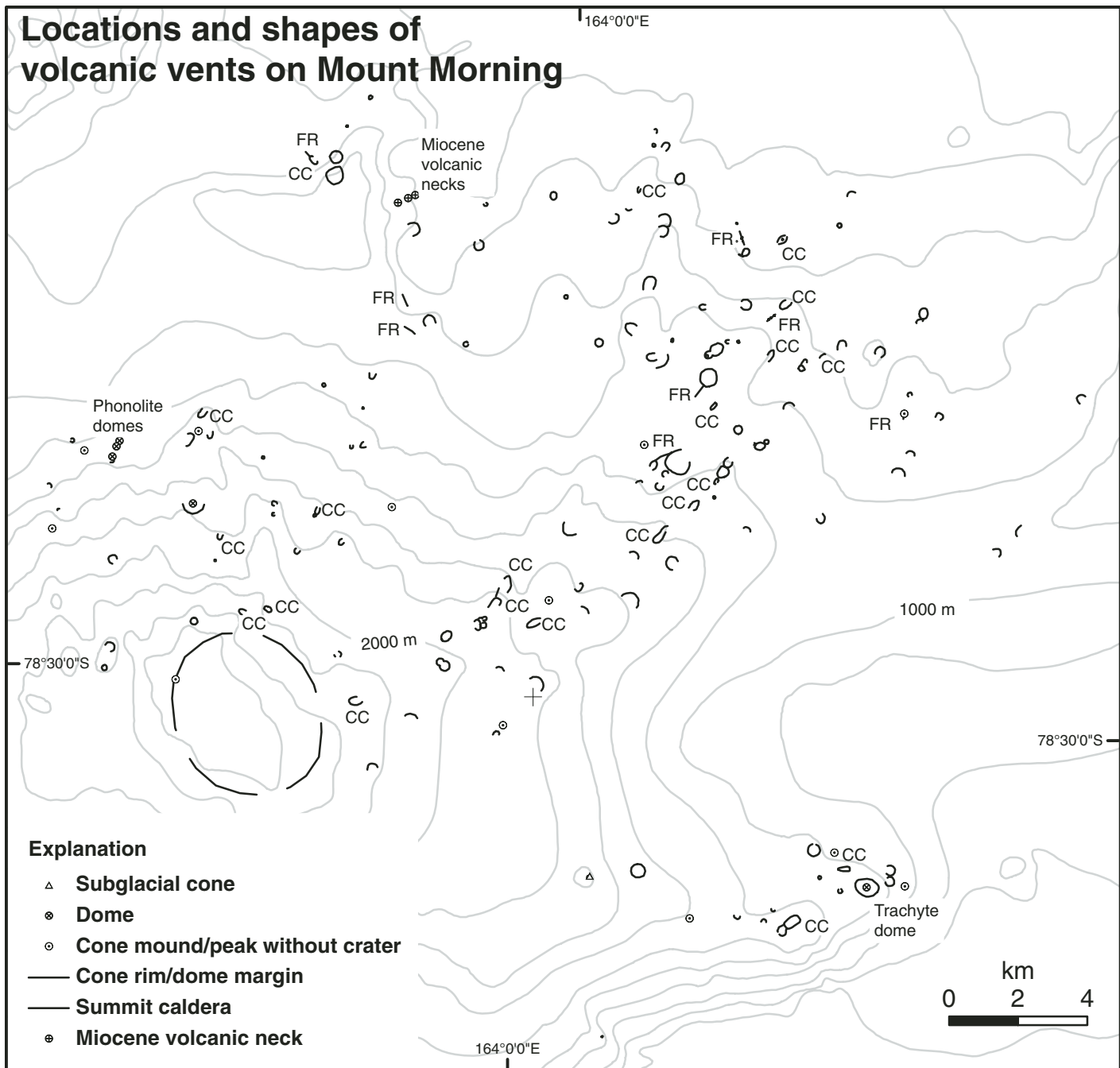


Figure 4. Topographic map of the Mount Morning area (same area as shown in Fig. 3) showing the locations and shapes of volcanic vents mapped in this study. In total, 186 vents were mapped on Mount Morning, most of which are basaltic cinder cones. Mount Morning's summit caldera is probably elongate in a NW direction, parallel to the elongate topography of the summit. FR—fissure ridge; CC—cleft cone.

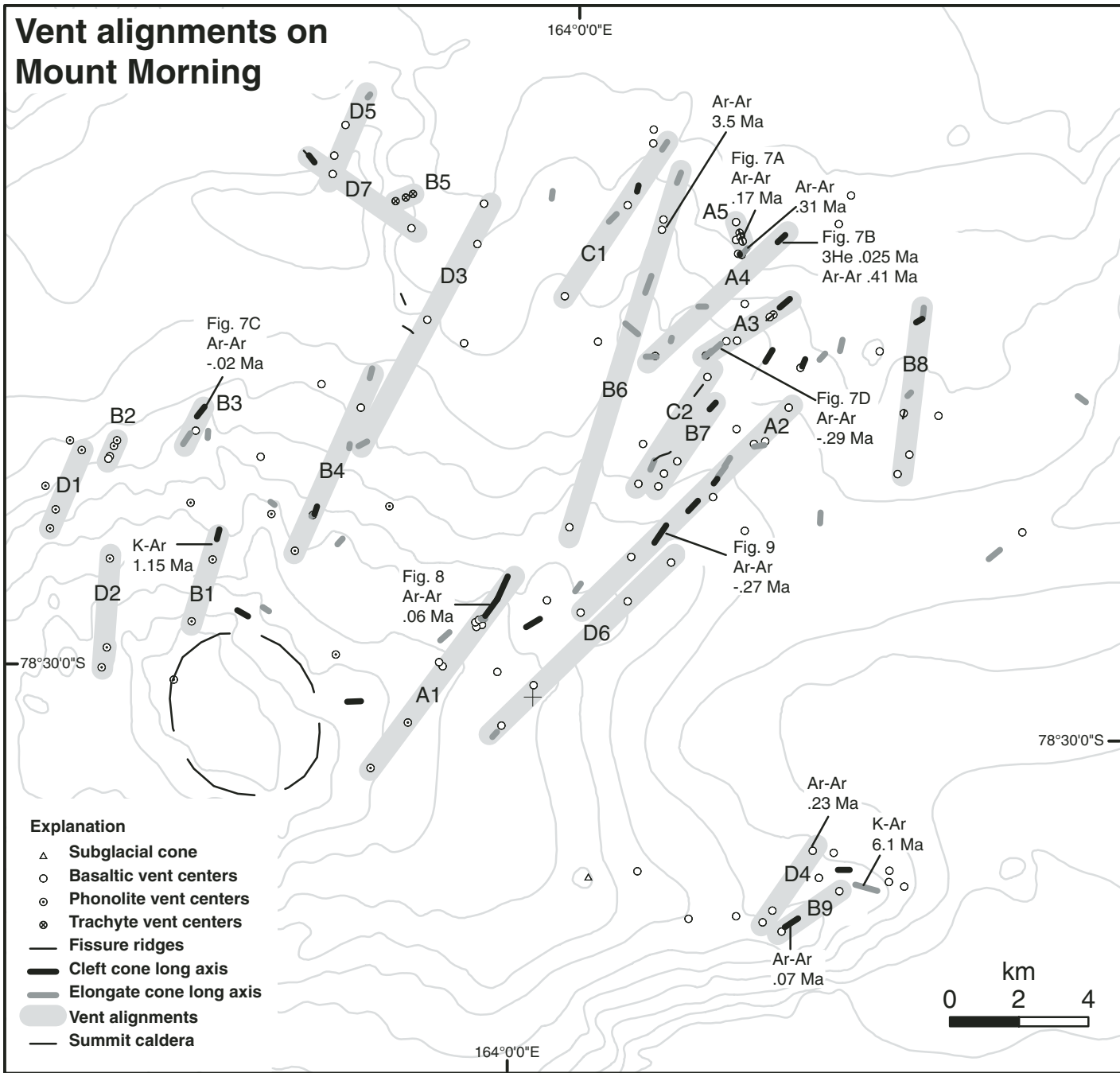


Figure 5. The majority of vent alignments on Mount Morning contain at least one fissure ridge, cleft cone, or elongate cone, which are directly related to the elongation direction of the subsurface fissure. Note that vent alignments trend predominantly NE, but there is a subsidiary NW trend. NE-trending alignments typically cross contour lines at a high angle. A, B, C, and D designate the quality rankings assigned to each alignment; see text for discussion.

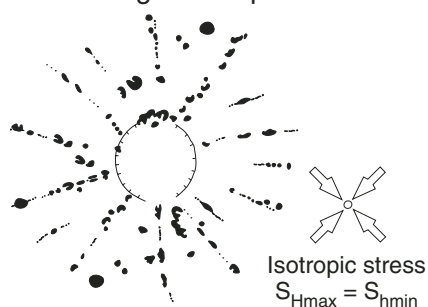
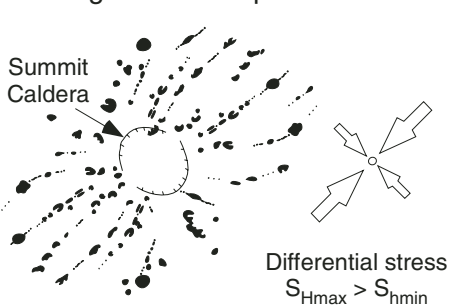
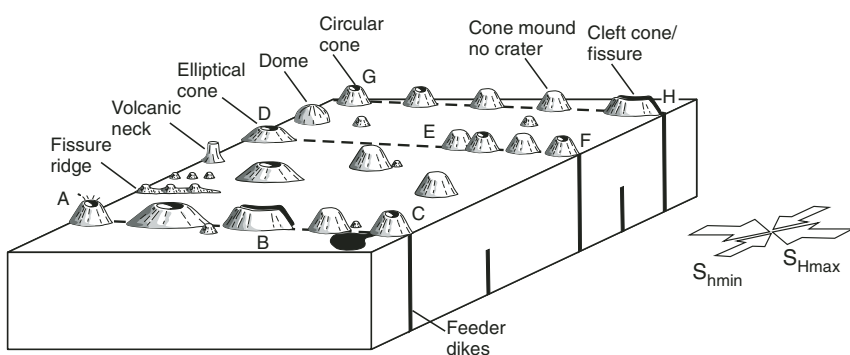
A Radiating fissure pattern**B Hourglass fissure pattern****C Elongate vents and vent alignments as indicators of fissure orientation**

Figure 6. Schematic models depicting fissure eruption patterns on polygenetic volcanoes in which hydraulic fracturing around the central conduit of the volcano leads to: (A) radial dikes and fissures in isotropic stress fields and (B) hourglass patterns in differential stress fields. Hydrostatic magma pressures within the central conduit dominate the stress field adjacent to it. Fissures show radiating patterns when close to the central conduit, but in a differential stress field, dikes and fissures curve to orientations parallel to S_h . Parasitic vents are after Chevallier and Verwoerd (1988). As shown in (C), fissures will express themselves as alignments of circular or elongate volcanic vents. Elongate landforms trend parallel to the subsurface trace of the fissure and can therefore be used to bolster the identification of vent alignments on a regional scale. Volcanic landforms are after Breed (1964). See text for discussion.

Previous studies of volcanic alignments as stress indicators have commonly mapped fissures based mainly on vent positions, connecting the center points of circular or elongate vents (e.g., Nakamura, 1977; Nakamura et al., 1977). For this study, we systematically exploit the fact that the elongation of vents is directly related to the elongation direction of their eruptive conduits (Breed, 1964; Tibaldi, 1995; Korme et al., 1997; Chorowicz et al., 1997; Adiyaman et al., 1998), providing a reliable indicator of local subsurface dike orientation and of vent alignments (Figs. 6C, 8A, and 9A). Our approach thus improves mapping of fissure orientations on a regional scale. We systematically mapped the locations and, wherever possible, the shapes of parasitic vents on Mount Morning. In order

to better constrain the age of basaltic cones and alignments, which make up the majority of the paleostress indicators, whole-rock ^{40}Ar - ^{39}Ar analyses were conducted on pyroclastic bombs, agglutinated spatter, and intercalated lava layers collected from basaltic cinder cones on Riviera Ridge, Hurricane Ridge, and Mason Spur. We summarize the main results of our mapping and age analyses next. Appendix 1 details the methodologies used to map vents, systematically distinguish elongate vents from circular vents, and map and rank vent alignments. Table A1 shows the detailed criteria utilized in the alignment ranking methodology. The methodologies used for the ^{40}Ar - ^{39}Ar analyses, which were conducted at the New Mexico Geochronological Research Laboratory, are reported along

with the analytical data in McIntosh and Esser (2005). Table 1 summarizes the results of the ^{40}Ar - ^{39}Ar analyses.

Results

Elongate Vents

We mapped a total of 186 parasitic vents on the flanks of Mount Morning that include cinder cones ($n = 170$), fissure ridges ($n = 8$), endogenous domes ($n = 5$), and volcanic necks ($n = 3$). In general, parasitic cones, domes, and necks ranged from a few meters to 0.7 km in diameter, and from a few meters to hundreds of meters in height (Wright-Grassham, 1987); fissure ridges ranged from 0.2 to 0.7 km in length. Elongate and cleft cones comprise 35% of the 170 cinder cones that we mapped; 37% of these were cleft cones, 13% had axial ratios ≥ 1.6 and < 1.8 , 23% had axial ratios ≥ 1.4 and < 1.6 , and 27% have axial ratios ≥ 1.2 and < 1.4 . Most of the cleft and elongate cones occur on Hurricane Ridge ($n = 43$), with fewer on Riviera Ridge ($n = 15$), and Mason Spur ($n = 2$). One trachyte dome on Mason Spur has an elongate shape, and the other four domes and three volcanic necks on Riviera Ridge have subcircular shapes. Fissure ridges occur on the lower slopes of the volcano on Riviera and Hurricane Ridges.

Our mapping and orientation analyses show three important results about elongate vents on Mount Morning. First, cleft and elongate cones predominantly have NNE- to NE-trending long axes (Figs. 4, 5, and 10B); 35 cones have long axes between $N20^\circ\text{E}$ and $N70^\circ\text{E}$, 12 cones have long axes between $N00^\circ\text{E}$ and $N19^\circ\text{E}$, and 5 cones have long axes between $N71^\circ\text{E}$ and $N90^\circ\text{E}$. Only eight cleft and elongate cones have NNW- to NW-trending long axes between $N13^\circ\text{W}$ and $N89^\circ\text{W}$. Four of eight fissure ridges also have NNE- to NE-trending long axes, whereas the remaining four ridges have NW-trending long axes (Fig. 10A). Second, fissure ridges, cleft cones, and elongate cones commonly have long axes that trend toward other cones, or are directly linked with other cones, some of which are also cleft or elongate cones with subparallel long axes (Figs. 4, 5, 7A, 8, and 9); this pattern is expected for vents that represent eruption from the same feeder dike. Thirdly, NNE to NE fissure ridges, cleft cones, and elongate cones trend at a high angle to contours on the volcano flanks, which suggests that the effects of the topographic slope of the volcano on the orientations of fissure eruptions were limited. Three of the eight WNW- to NW-trending elongate cones occur at high elevations (> 1800 m) proximal to the rim of the volcano where they parallel contours on the volcano slope. The remaining five NW-trending elongate cones occur at lower

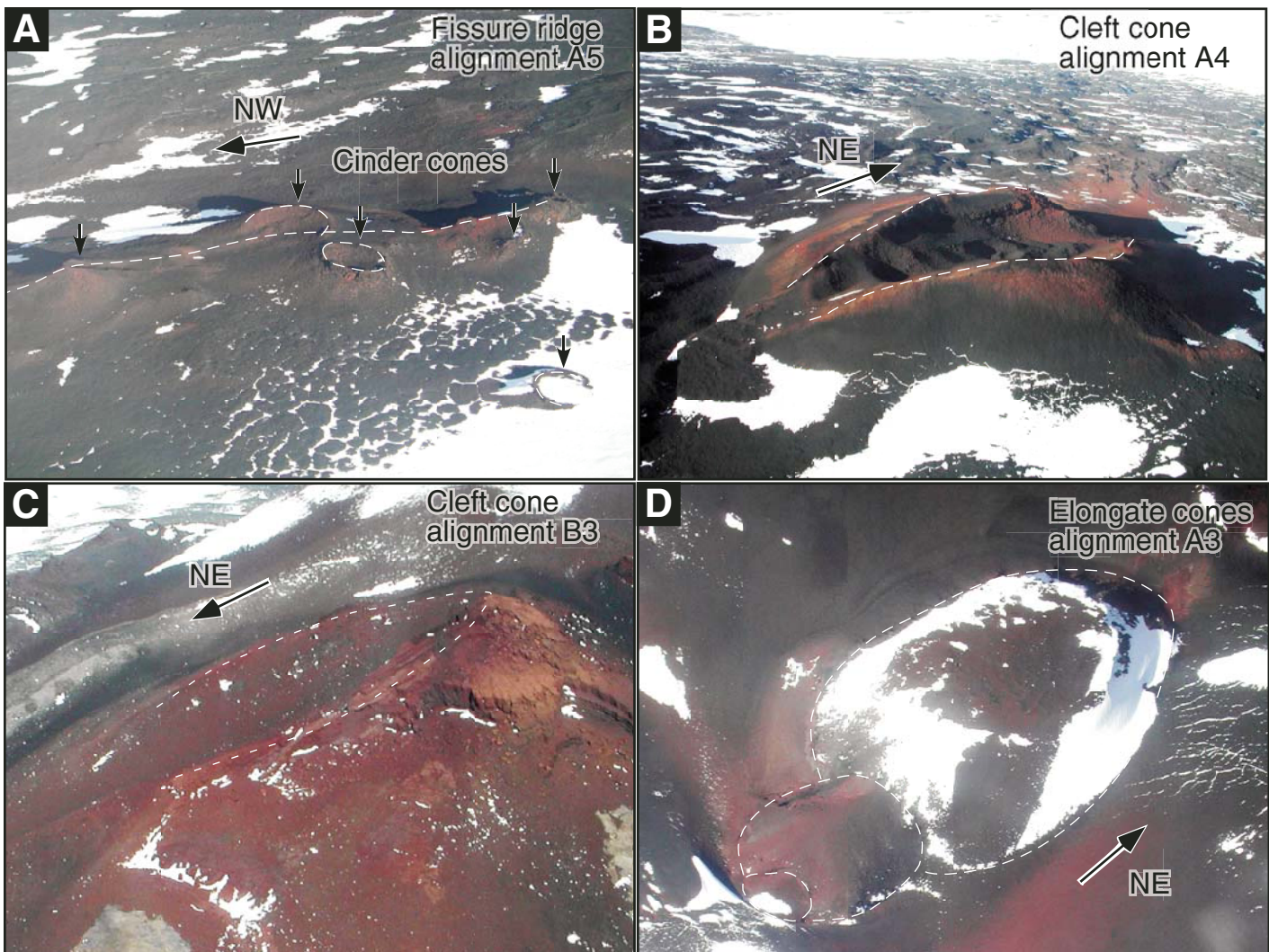


Figure 7. (A) Photo of an ~0.25-km-long basaltic NW-trending fissure ridge that connects small cinder cones. Several small cones occur along the projection of the fissure ridge, indicating that they collectively form a vent alignment (alignment A5 in Fig. 5). (B) Photo of an ~0.3-km-long basaltic NE-trending cleft cone showing smaller circular craters aligned within the NE-trending cleft crater. Informal name is Emperor Cone (after Kurz and Ackert, 1996). Several cones occur along the SW projection of the long axis of the cleft cone, indicating that they collectively form a vent alignment (alignment A4 in Fig. 5) along the same feeder dike. (C) Photo of an ~0.25-km-long basaltic NE-trending cleft cone on Riviera Ridge that is breached to the northeast and part of vent alignment B3 (Fig. 5). (D) Photo of an ~0.6-km-long alignment of three basaltic cones that coalesce in a NE direction; two of the cones are elongate NE. A NE-trending cleft cone and fissure ridge occur along the northeast projection of these elongate cones, indicating that they collectively formed along the same NE-trending fissure (alignment A3 in Fig. 5).

elevations, and four of these are locally subparallel to contours on the volcano slope. All of the NNE to NE fissure ridges trend at a high angle to contours on the volcano flanks, whereas three of the four WNW to NW fissure ridges are subparallel to contours.

Vent Alignments

Since vent shapes carry critical information about the orientation of the subsurface feeder dike, we defined vent alignments by (1) linking vents that lie close to and along the trend

of the long axis of fissure ridges, cleft cones, or elongate cones, since these types of vents can be directly related to the trend of subsurface fissures, and by (2) linking vents that, because of their close spacing and/or coalescence, occur in clear visual alignments. Identified alignments were grouped into four quality rankings, where A > B > C > D. The higher the ranking, the higher our confidence is that an alignment actually marks a subsurface feeder dike. Our alignment analysis identified a total of 23 vent alignments that range from 0.6 to 7.8 km in length

and these include: (1) five A-ranked alignments (A1–A5) on Hurricane Ridge; (2) nine B-ranked alignments (B1–B9) on Riviera Ridge, Hurricane Ridge, and Mason Spur; (3) two C-ranked alignments (C1 and C2) on Hurricane Ridge; and (4) seven D-ranked alignments (D1–D7) on Riviera Ridge, Hurricane Ridge, and Mason Spur. Table A2 lists each of the alignments, along with their rank and relevant dimensional and statistical data.

Vent alignments on Mount Morning defined by our mapping have several key characteristics.

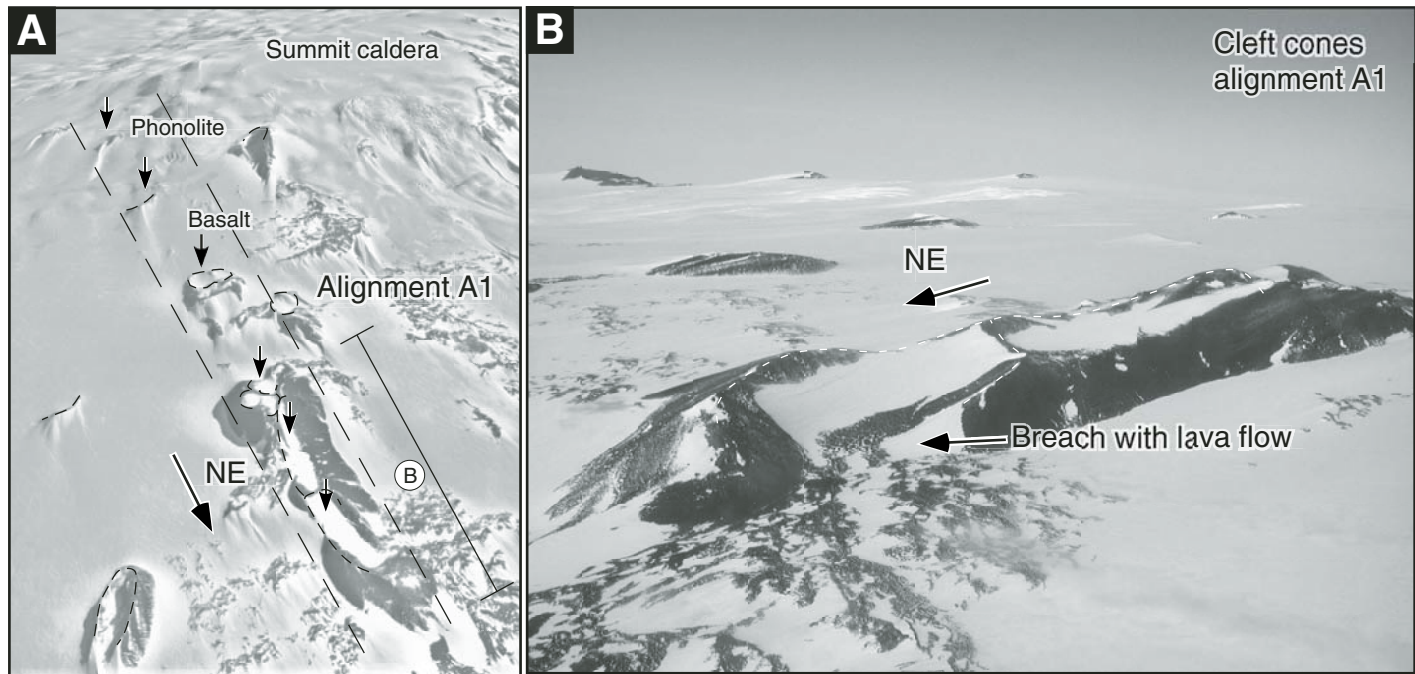


Figure 8. Aerial photographs showing (A) vent alignment A1 and (B) two basaltic cleft cones (upper Hurricane Ridge; Fig. 5). The long axes of the cleft cones mark the subsurface feeder dike trend and cones that occur along the projection of their long axes, likely erupted from the same feeder dike. The two southern cones in the alignment are phonolitic in composition, indicating that they erupted at a separate time with respect to the basaltic cones in the alignment to the north. The phonolitic cones either did not erupt from the same fissure or basaltic magmatism may have reactivated the same fissure utilized by phonolitic magmatism. Alignment A1 in A is ~6.5 km long. The two cleft cones in B have an overall length of 1.3 km.

First, vent alignments predominantly trend NE (Figs. 5 and 10C). The highest quality alignments A1–A4 have azimuths that range from N37°E to N58°E, and alignment A5 has a N19°W azimuth. Alignments B1–B9 have azimuths that range from N7°E to N67°E. Alignments C1–C2 have ~N34°E azimuths. Alignments D1–D6 have azimuths that range from N4°E to N46°E, and alignment D7 has a N55°W azimuth. Second, like the long axes of individual elongate cones, NNE- to NE-trending vent alignments typically trend at a high angle to contours on the flanks of the volcano, which, as is the case with elongate vents, suggests that the effects of the topographic slope of the volcano on the orientations of fissure eruptions were limited. Thirdly, the majority of the vent alignments ($n = 20$) are monocompositional, which is expected for alignments that represent synchronous eruption from the same feeder dike. Sixteen of the alignments exclusively consist of basaltic vents (Figs. 2 and 5; Table A2), three alignments (B1, D1, and D2) are composed of phonolitic vents, and one alignment (B5) is made up of trachytic volcanic necks. The remaining three alignments (A1, B2, and B4) are a mix of phonolitic and basaltic vents, suggesting local reactivation of previously formed fractures during diachronous

volcanism. Finally, as illustrated by Figure 5, several of the NNE- to NE-trending alignments (A1, A2, B6, B8, C1, and D6) locally manifest themselves as ridges on the volcano slope, which is a common topographic manifestation of fissure eruptions.

Ages of Vents

Previous Work. The oldest vents that we have mapped occur in alignment B5, which consists of volcanic necks within the Miocene (18.7–14.6 Ma K-Ar) subvolcanic complex on Riviera Ridge (Figs. 2, 4, and 5) (Kyle and Muncy, 1989). K-Ar analyses yielded an age of 6.1 Ma for trachytic rocks from the WNW elongate trachyte dome on top of the Miocene volcanic complex on Mason Spur (Fig. 5) (Wright-Grassham, 1987). K-Ar analyses of four phonolitic rocks from the upper slopes of Mount Morning have ages ranging from 1.0 to 1.2 Ma (Polyakov et al., 1976; Armstrong, 1978; Stuiver and Braziunas, 1985); one of these samples (1.15 Ma K-Ar; see Fig. 5) was collected from the upper slopes of the volcano and is the only sample for which the collection locality is known. The K-Ar ages indicate that phonolitic vents and alignments are as young as the Pleistocene (Polyakov et al., 1976; Armstrong, 1978), consistent with the undis-

sected nature of the phonolitic rocks that comprise the summit volcano (Wright-Grassham, 1987; Wright and Kyle, 1990a).

Field relations suggest that basaltic vents and alignments postdate phonolitic volcanism (Wright-Grassham, 1987), which is consistent with 220–25 ka ^{39}Ar surface exposure ages (Kurz and Ackert, 1996) for basaltic lavas on the lower northern flank of Mount Morning on Hurricane Ridge (e.g., Figs. 5 and 7B; alignment A4). Based on these field relations, Wright-Grassham (1987) viewed older 2.2–2.4 Ma K-Ar ages reported by Polyakov et al. (1976) for basalts from Mount Morning (sample locations unknown) as being in error. A Pleistocene age for basaltic volcanism is also suggested by the unweathered appearance of the basaltic cinder cones (Figs. 7, 8, and 9), which has led previous authors to suggest that the basaltic cones may be as young as late Pleistocene (<100 ka; Wright-Grassham, 1987; Kyle and Muncy, 1989; Wright and Kyle, 1990b).

^{40}Ar - ^{39}Ar Analyses. The ^{40}Ar - ^{39}Ar mineral ages were calculated relative to the Fish Canyon sanidine (28.02 Ma; Renne et al., 1998; McIntosh and Esser, 2005), and they are listed in Table 1. The results can be divided into three types (herein referred to as types 2–4 to remain consistent with McIntosh and Esser, 2005)

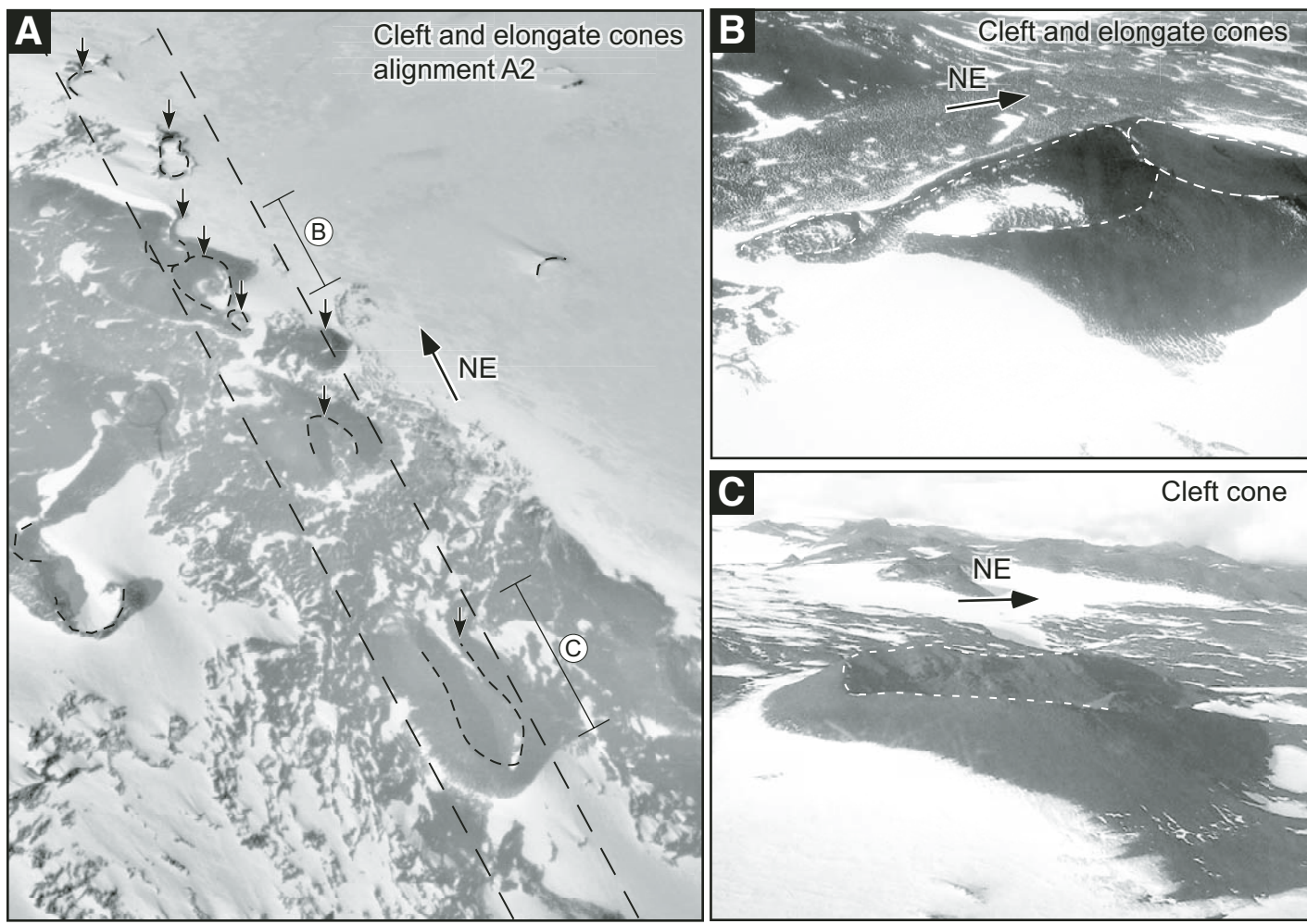


Figure 9. (A–C) Aerial photographs of basaltic cinder cones on Hurricane Ridge showing several cinder cones that are elongate in a NE direction (alignment A2; Fig. 5). The elongated cone long axes are parallel and along the same trend, suggesting that they mark a vent alignment related to fissure eruption above a single NE-trending subsurface feeder dike a minimum of ~6 km in length. The cleft cones in B and C are ~0.6 and 0.8 km in length, respectively.

TABLE 1. SUMMARY OF $^{40}\text{Ar}/^{39}\text{Ar}$ RESULTS FROM GROUNDMASS CONCENTRATES

Quality Sample	Alignment	Material	Max % $^{40}\text{Ar}^*$	Analysis	n	% ^{39}Ar	MSWD	Preferred age (Ma)		K/Ca	Age (Ma)	\pm	2σ
								$^{40}\text{Ar}/^{36}\text{Ar}$	\pm				
<i>Type 2</i>													
55298-01	A5	Basalt	5	Isochron	7		1.3	304	\pm 3	1.0	0.17	\pm	0.10
55290-01	NE Cone	Basalt	3	Plateau	6	67.3	1.3	296	\pm 4	0.2	0.31	\pm	0.08
55302-01	B3	Basalt	2	Isochron	5		1.8	298	\pm 8	0.4	-0.02	\pm	0.02
<i>Type 3</i>													
55288-01	B6	Basalt	14	Plateau	8	87.3	2.7	297	\pm 5	0.2	3.50	\pm	0.20
55158-01	D4	Basalt	3	Isochron	6		0.9	300	\pm 3	0.4	0.23	\pm	0.22
55151-01	B9	Basalt	4	Isochron	6		0.8	301	\pm 2	0.4	0.07	\pm	0.08
55286-01	A2	Basalt	2	Isochron	6		0.7	303	\pm 3	0.7	-0.27	\pm	0.22
<i>Type 4</i>													
55308-01	A1	Basalt	6	Isochron	6		0.5	298	\pm 3	0.5	0.06	\pm	0.08
55306-01	A4	Basalt	2	Plateau	5	61.8	6.1	302	\pm 7	0.3	0.41	\pm	0.39
55300-01	A3	Basalt	2	Isochron	4		1.9	300	\pm 8	0.6	-0.29	\pm	0.36

Notes: Results are divided into types (type 2—highest quality) based on age spectra and isochrons, as detailed in McIntosh and Esser (2005). Max % $^{40}\text{Ar}^*$ is maximum radiogenic yield, excluding imprecise initial and final heating steps; n is number of heating steps used in weighted-mean of isochron age; % ^{39}Ar is percent of total ^{39}Ar used in weighted-mean age calculation; $^{40}\text{Ar}/^{36}\text{Ar}$ is isochron intercept. MSWD—mean square of weighted deviates.

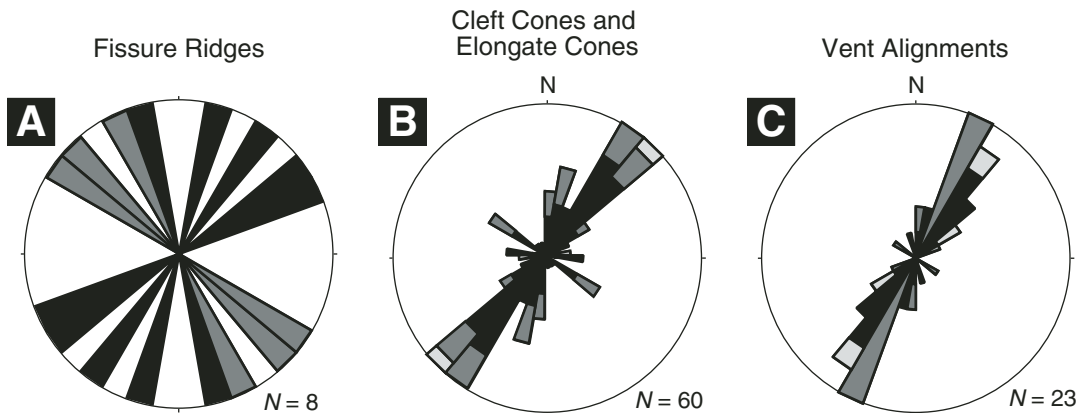


Figure 10. Symmetric rose diagrams of (A) fissure ridges (outer circle = 13%); (B) cleft and elongate cones (outer circle = 20%); and (C) vent alignments (outer circle = 26%) with black, dark gray, and light gray representing Hurricane Ridge, Riviera Ridge, and Mason Spur, respectively. Fissure ridges have NE and NW trends. Most cleft cones, elongate cones, and vent alignments trend NE, but there is a subsidiary NW cone and alignment trend.

based on the type of spectrum and isochron (McIntosh and Esser, 2005). Type 2 samples have well-developed spectra or isochrons, reasonably precise ages for individual heating steps (± 0.05 – 0.22), and smaller age uncertainties (± 0.02 – 0.10) (McIntosh and Esser, 2005). Type 3 samples have lower-quality spectra or isochrons, lower precision in ages for individual heating steps (typically ± 0.14 – 0.63), and larger age uncertainties (± 0.08 – 0.22) than type 2 samples (McIntosh and Esser, 2005). Type 4 results typically have even lower-quality spectra or isochrons, lower precision ages for individual heating steps (typically ± 0.10 – 0.45), and larger age uncertainties (± 0.06 – 0.39) than type 3 samples (McIntosh and Esser, 2005). Sample types 2, 3, and 4 yielded ages ranging, respectively, from effectively zero (isochron) to 0.31 ± 0.08 Ma (plateau), zero to 3.5 ± 0.2 Ma (plateau), and zero to 0.41 ± 0.39 Ma (plateau) (McIntosh and Esser, 2005). The 0.41 ± 0.39 Ma type 4 plateau age (55306–01) is within analytical error of a 0.025 ± 0.03 Ma ^3He surface exposure age for lava flows from the same vent (Kurz and Ackert, 1996), which suggests the ^{40}Ar - ^{39}Ar mineral ages accurately record eruption ages within the analytical error of the analyses.

Figure 5 shows the ages with respect to the vent alignments. Cones within A-ranked alignments yielded ages of 0.06 ± 0.08 Ma (A1), -0.27 ± 0.22 Ma (effectively zero; A2), -0.29 ± 0.36 Ma (effectively zero; A3), 0.17 ± 0.10 Ma (A5), and 0.41 ± 0.39 Ma (A4) (McIntosh and Esser, 2005). Cones within B-ranked alignments yielded ages -0.02 ± 0.02 Ma (effectively zero; B3), -0.07 ± 0.08 Ma (effectively zero; B9), and 3.5 ± 0.2 Ma (B6) (McIntosh and Esser, 2005).

A cone within D-ranked alignment D4 yielded an age of 0.23 ± 0.22 Ma. One NE elongate cone on Hurricane Ridge that does not occur within a cone alignment yielded an age of 0.31 ± 0.08 Ma (McIntosh and Esser, 2005).

DISCUSSION AND CONCLUSIONS

Crustal Stress Field at Mount Morning

Structural analyses and whole-rock ^{40}Ar - ^{39}Ar cooling ages of parasitic elongate vents and vent alignments indicate that, during the Pleistocene, flank eruptions on Mount Morning systematically occurred along NE-trending fissures, with a minor amount of coeval volcanism along a subsidiary NW trend. Figures 5 and 10 show that vent alignments predominantly trend NE, regardless of their position around the summit caldera. This is contrary to the radial pattern predicted if an isotropic stress field characterized the Mount Morning area when the fissures formed (Fig. 6A) (Nakamura, 1977; Nakamura et al., 1977). The linear traces of elongate vents and vent alignments on topography also show that the local effects of the volcano on the orientations of fissure eruptions were limited. Volcano topography, magma chamber shape and pressures, and/or surface loading can generate a minimum horizontal stress (S_h) parallel to the local topographic slope of the volcano, causing elongate vents and vent alignments to form roughly parallel to major topographic contours on the flanks of the volcano (Simkin, 1972; Chadwick and Howard, 1991; Chadwick and Dieterich, 1995). Such factors may explain elongate vents near the summit caldera rim and

vent alignment B9 on Mason Spur, which trend subparallel to local topography, but they do not explain the bulk of the elongate vents and vent alignments on Mount Morning.

It is important to assess the degree of control on the vent alignments at Mount Morning by underlying structure, including Paleozoic basement fabrics within the Ross orogen and the rift-related Cenozoic Transantarctic Mountains Front fault zone. The structure beneath Mount Morning is poorly known because the surrounding Ross Ice Shelf cover has impeded seismic investigations, and the mantle of ice and young volcanics over the volcano leaves the basement exposed at only a single locality at the northwest tip of Hurricane Ridge (Gandalf Ridge, Fig. 2). There, a small exposure of Paleozoic basement granite and metasedimentary rocks was mapped by Muncy (1979), but no basement structure was recorded. Structural trends in the Ross orogen basement of the Transantarctic Mountains to the west of Mount Morning, however, have a dominant NW-SE trend (Findlay et al., 1984; Cook and Craw, 2001) at a high angle to the NE vent alignments. Dikes within the Miocene subvolcanic complex at Gandalf Ridge trend E-W, and N-S faults, possibly rift-related, cut both the basement and Miocene volcanic rocks and dikes (Muncy, 1979; Kyle and Muncy, 1989). This local evidence suggests that structures beneath the Pleistocene Mount Morning volcano are at oblique angles to the NE vent alignment trends. On the regional scale of the entire Erebus Volcanic Province, there is no systematic arrangement of major volcanoes along or parallel to the trend of the Transantarctic Mountains Front fault zone (Figs. 1 and 11). Individual shield and stratovol-

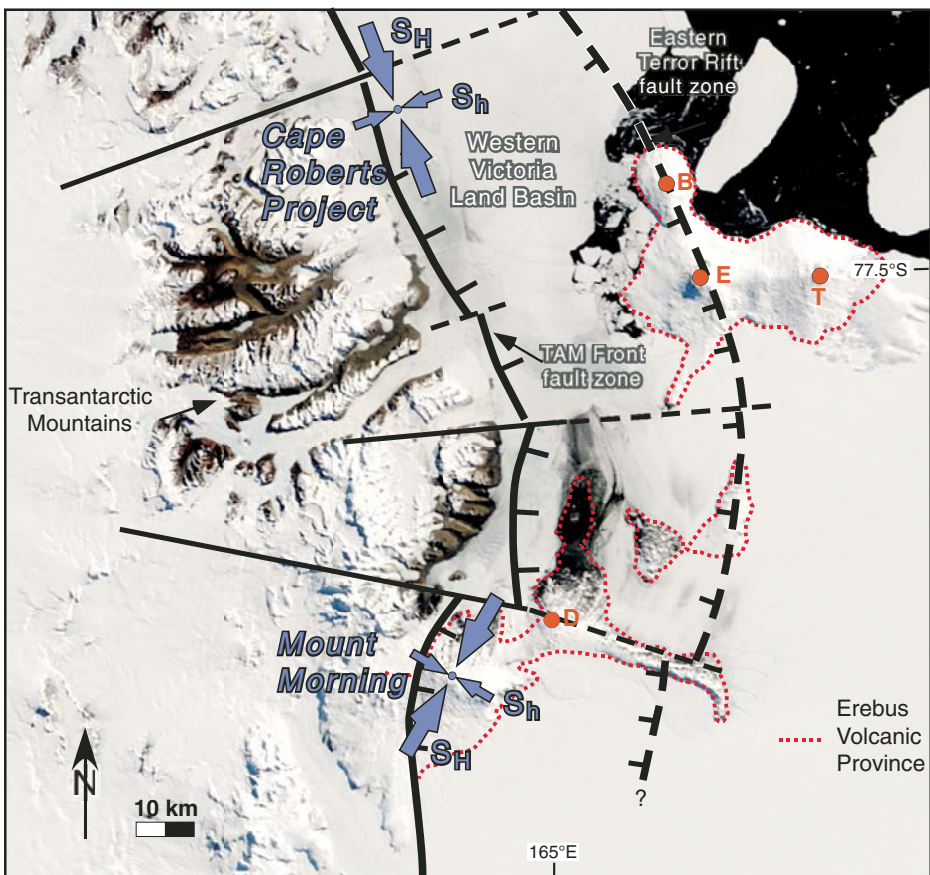


Figure 11. Moderate Resolution Imaging Spectroradiometer satellite image showing S_h directions with respect to the major structural and volcanic elements of the Erebus Volcanic Province in the western Victoria Land rift basin. The NE S_h direction indicated by volcanic alignments on Mount Morning is rotated clockwise with respect to the NNW S_h direction determined from borehole breakouts and drilling-induced fracture studies of the Cape Roberts drilling project. The S_h direction appears to track the Transantarctic Mountains (TAM) frontal fault zone, the western border fault of the rift system. Rift structure is after Wilson (1999) and Hall et al. (2007). D—Mount Discovery; E—Mount Erebus; T—Mount Terror; B—Mount Byrd.

canoes are not highly elongated, in contrast to the Hallett Volcanic Province in northern Victoria Land, where the Adare, Hallett, and Daniell Peninsulas and Coulman Island mark ~N-S, highly elongate shield volcano complexes aligned along the Transantarctic Mountains Front–rift boundary (Fig. 12) (McIntosh and Kyle, 1990). Instead, Erebus Volcanic Province emergent volcanoes, as well as submarine volcanic edifices documented by aeromagnetic data, are concentrated in a zone extending eastward at a high angle to the Transantarctic Mountains Front, potentially recording volcanism along a transfer fault zone in the rift (Damaske et al., 1994; Behrendt et al., 1996; Chiappini et al., 2002). The limited data available do not allow us to entirely rule out control by rift structures, but they do indicate that the locations and shapes of

major volcanoes in the Erebus Volcanic Province are not aligned along rift-parallel structures and that the NE vent alignments at Mount Morning are oblique to both basement structure and local faults that may be rift-related. We therefore favor the simplest scenario for the systematic NE fissure eruptions, in which repeated magmatically induced hydraulic fracturing of the volcanic edifice formed vent alignments in a NE direction because of the presence of a differential stress field in which S_h trends NE (Nakamura, 1977; Nakamura et al., 1977).

Delaney et al. (1986) showed that preexisting structures must strike at a high angle to the S_h direction to accommodate an intrusion. Only in a region where the stress field is either isotropic or characterized by very low differential stress will a broad azimuth range of preexisting struc-

tures be reactivated as magma conduits. Drilling-induced fractures in core and borehole walls at Cape Roberts, to the north of Mount Morning, document a high horizontal stress difference in this sector of the rift system (Moos et al., 2000; Wilson and Paulsen, 2000; Jarrard et al., 2001; Wilson and Paulsen, 2001). At Mount Morning, there is a strong predominance of NE-trending fissures, regardless of position around the summit caldera, which is again inconsistent with an isotropic stress field or a low differential stress. Thus, if basaltic magmatism at Mount Morning did reactivate preexisting magmatically induced fractures or older basement fractures, the error associated with using the fissures as stress indicators should be negligible.

The majority of the NE vent alignments cannot be projected linearly back to the summit caldera, which is consistent with a fissure swarm controlled by the regional stress field rather than a radial swarm. The fissures could possibly curve to radial orientations near the summit caldera, where the hydrostatic influence of the magma within the central conduit controls dike propagation (Fig. 6B) (Muller and Pollard, 1977; Nakamura, 1977), but no such pattern is clearly defined by our mapping in the largely ice-covered summit region.

The ^{40}Ar - ^{39}Ar analyses reported herein, along with previously reported K-Ar and ^3He surface exposure ages, bracket the timing of parasitic volcanism and the time span over which a regional NE S_h stress direction controlled the orientation of fissure eruptions on Mount Morning. Nine of the ten ^{40}Ar - ^{39}Ar ages reported herein range from effectively zero to 0.41 Ma, indicating that the parasitic cones on Mount Morning represent some of the youngest cones yet identified outside of Mount Erebus in the Erebus Volcanic Province; one age (3.5 ± 0.2 Ma; alignment B6) falls outside this range. Although ^{40}Ar - ^{39}Ar results from alignment B6 (type 3) are less precise than those samples with type 2 ages, the fact that their ages differ by more than ten times the sum of their analytical errors suggests that the sample from B6 was indeed erupted significantly earlier (McIntosh, 2006, personal commun.). Together with other age data, these results show that all but three of the alignments are of Pleistocene age. NE-trending alignment B6 has a Pliocene age, and the WNW elongate trachyte dome on Mason Spur (6.1 Ma K-Ar) and the three volcanic necks that make up vent alignment B5 on Riviera Ridge (Fig. 5) are of Miocene age. The overall consistency of the preferred ^{40}Ar - ^{39}Ar ages reported herein suggests that much of the basaltic cinder cone volcanism on Mount Morning and Mason Spur occurred in the Pleistocene after parasitic phonolitic volcanism (1.0–1.2 Ma

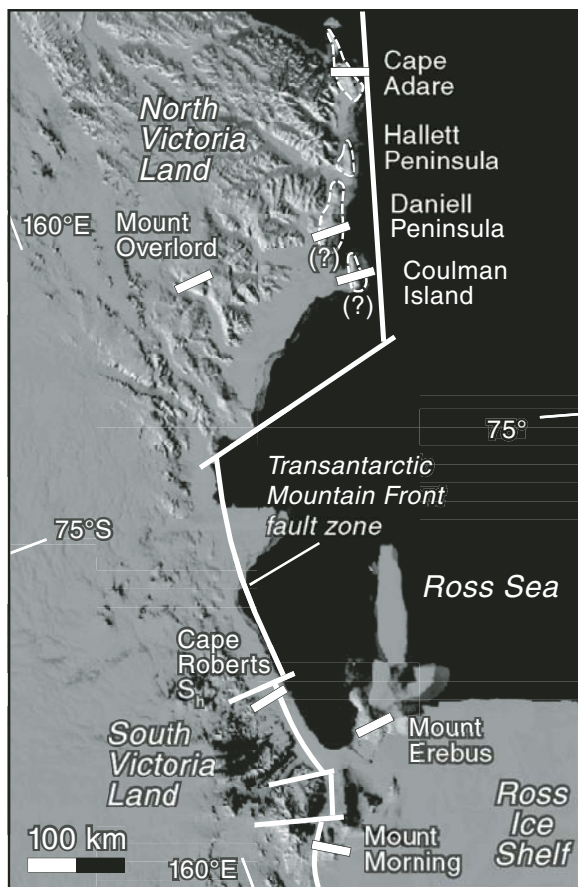


Figure 12. MODIS image showing S_h directions (white bars) interpreted from volcanic alignments on Mount Morning, borehole and core fractures at Cape Roberts, and the elongation directions of summit calderas in the McMurdo Volcanic Group along the western flank of the West Antarctic Rift system (modified from Paulsen and Wilson, 2007; image mosaic from Haran et al., 2005). Note that the majority of the elongation directions of calderas are parallel to the contemporary S_h direction documented by borehole and core fractures at Cape Roberts.

a N31°E Pliocene to Pleistocene S_h direction (15° standard deviation). Exclusion of D-ranked vent alignments from this calculation does not significantly affect the results (N33°E azimuth; 15° standard deviation). The 2008 World Stress Map quality ranking system for a “stress datum” derived from volcanic vent alignment data is based on the numbers of alignments and their degree of parallelism (evaluated by their standard deviation; Heidbach et al., 2008). Using these criteria, the N31°E S_h direction derived from all of the NE Pliocene to Pleistocene vent alignments achieves a B quality rank. The B quality rank for the stress datum is a consequence of the standard deviation, which is 3° above the 12° threshold for an A quality rank. This problem is mitigated and a higher quality rank is achieved when the vent alignments with large magnitudes of deviation ($\geq 24^\circ$) from the average are excluded (a total of four vent alignments). In this case, the NE Pliocene to Pleistocene vent alignments yield a N31°E S_h direction (10° standard deviation), which achieves an A quality ranking. We consider the N31°E S_h direction to be the most accurate estimate of the regional stress field because vent alignments have lengths on the order of several kilometers (versus tens to hundreds of meters for elongate cones) and thus record the orientation of the principal stresses over greater volumes of crust. Because the fissure eruptions occurred over an extended time interval, this can be considered a long-term stress pattern for the Pleistocene and possibly part of the Pliocene.

The elongate shape of Mount Morning’s summit caldera lends support for a Pleistocene differential stress field with NE S_h in the region. The caldera rim shown in Figure 4 is 4.9 km long, 4.1 km wide, and is similar in both location and shape to the summit caldera previously mapped by Wright-Grassham (1987). Rock outcrops define the rim on the NW, SW, and S sides, but the exact location of the NE rim of the caldera is obscured by snow cover. A more northwesterly elongation direction for the caldera may be indicated by the WNW elongated topography of the summit. Many of Earth’s major Pleistocene volcanoes have elongate summit calderas with long axes perpendicular to volcanic alignments on their flanks and to the regional S_h direction, determined by independent means (Fig. 6B) (Bosworth et al., 2000, 2003; Holohan et al., 2005). Mount Morning shows an intriguing similarity to these volcanoes. The summit caldera is elongate to the NW at a high angle to NE fissures that dominate the volcano’s flanks. Bosworth et al. (2003) suggested that crustal stress fields cause instabilities in the walls of a magma chamber, causing the walls to spall off, as is the case with

K-Ar; Polyakov et al., 1976; Armstrong, 1978). Alignments that contain both phonolitic and basaltic vents (A1, B2, B4) would thus require Pleistocene basaltic magmatism to have locally reactivated previously formed fractures induced during phonolitic volcanism. Changes in the magnitudes of the regional stresses with respect to magmatic pressures could explain the transition from the earlier eruptions of more-evolved phonolitic magmas to more recent eruptions of less-evolved basaltic magmas by promoting a more rapid magma ascent along NE-trending fractures and consequently smaller crustal residence times (cf. Haug and Strecker, 1995; Franz et al., 1997), but present data are insufficient to test this model. Overall, the age data and alignment orientations demonstrate a NE-trending S_h in the Pleistocene, and age data from one alignment suggests that this regime may date back to the Pliocene.

The resolution limits of the ^{40}Ar - ^{39}Ar age analyses of the sampled basaltic volcanic rocks preclude us from assessing the relationship of NE- and NW-trending fissure eruptions through time. NW elongate vents that trend subparallel to contour lines on the volcano’s upper flanks (Figs. 4 and 5) probably owe their orientation to stresses

generated locally due to volcano topography and/or magma chamber shape. NW-trending vent alignments A5 and perhaps D7 may record local variation of the stress direction related to such factors or, alternatively, to stress field rotation caused by dike inflation along the main NE fissure trend (Parsons and Thompson, 1991).

Fissures on the flanks of volcanoes show a range of trends, even in cases where their orientation has been governed by a regional differential stress field. This occurs because of mechanical heterogeneities in the country rock, the proximity of a fissure to the central conduit of the volcano, and possible changes in the regional stress field over the time of volcanism (Nakamura, 1977). The range in NE azimuths of elongate vents and vent alignments on the flanks of Mount Morning should be distributed around the average trend of the dominant regional S_h direction during the Pliocene to Pleistocene. An average of the azimuths of the elongate vents indicates a N31°E S_h direction (52° standard deviation), whereas an average of only the NE elongate vents indicates a N39°E S_h direction (22° standard deviation). An average of the orientations of all of the NE Pliocene and Pleistocene vent alignments suggests

borehole breakouts, and create a magma chamber elongate in the direction perpendicular to $S_{H'}$. Subsequent roof collapse associated with the evacuation of an elongate magma chamber leads to an elongate caldera. Analogue models suggest that elongate calderas can also develop perpendicular to S_H because of the effect of the stress field on ring fracture orientations (Holohan et al., 2005). The Mount Morning summit caldera must be younger than the volcano itself, which Wright-Grassham (1987) estimated to be no older than 2.5 Ma based on K-Ar ages, and it could be younger than the 1.0–1.2 Ma phonolitic volcanic rocks that probably mark the latest volcanism associated with the growth of the central volcano (Wright-Grassham, 1987). Regardless of the exact caldera elongation mechanism, the elongated summit topography and the mapped elongate summit caldera on Mount Morning indicate a N30°E to N60°E Pliocene to Pleistocene S_H direction, which is similar to the N31°E S_H direction indicated by the vent alignments.

Implications for Contemporary Stress in the West Antarctic Rift System

Considering the young age for parasitic volcanism on Mount Morning and the dominance of NE fissure eruptions for a significant period of the Pleistocene, the N31°E S_H direction indicated by the vent alignments likely reflects the contemporary S_H direction for the Mount Morning area. This N31°E S_H direction is at an angle to the contemporary N13°W and N15°W S_H stress directions determined from borehole breakouts and drilling-induced fractures in boreholes and cores from the Cape Roberts Project ~100 km to the north of Mount Morning (Fig. 11) (Moos et al., 2000; Wilson and Paulsen, 2000; Jarrard et al., 2001; Wilson and Paulsen, 2001). Regionally, this N31°E S_H direction is also at an angle to the NNW S_H direction defined by regionally consistent ENE elongation directions of Miocene and Pleistocene elongate summit calderas in the McMurdo Volcanic Group in the western Ross Sea, which appear to record similar orientations for S_H since ca. 7 Ma (Fig. 12; Paulsen and Wilson, 2007).

A striking parallelism between the S_H direction and the trend of the rift boundary emerges when our new Mount Morning datum is compared with the borehole results at Cape Roberts (Fig. 11). The architecture of the Transantarctic Mountains Front border fault zone between the rift and the uplifted rift flank is modeled as a series of west-tilted fault blocks segmented by transverse structures (e.g., Fitzgerald, 1992, 2002; Wilson, 1999). The S_H stress direction defined by the Mount Morning vent alignments is rotated clockwise relative to the in situ

stress directions at Cape Roberts, in the same region where the rift border fault is inferred to change trend and step westward across a regional accommodation zone (Wilson, 1999). Thus, the S_H stress directions at both Cape Roberts and Mount Morning are consistently oriented subparallel to the inferred trace of the rift-flank boundary, changing along the trend of the rift system. In contrast, contemporary and paleostress indicators in rifts within other continents typically show homogeneous S_H directions, regardless of rift-flank trend (Illies and Greiner, 1978; Golembek et al., 1983; Strecker et al., 1990; Ring et al., 1992; Mortimer et al., 2007). Several hypotheses can explain the stress pattern we observe. First, one of the stress orientations may simply mark a local anomaly within a homogeneous stress field. The orientation change of ~45° is substantial, but is similar to a local orientation change in the stress field around the Rhine graben, where recent stress release is inferred to have altered the regional stress orientation (Illies et al., 1981). Second, the orientation of S_H defined by the vent alignments at Mount Morning may deviate from the regional orientation due to structural control. As previously discussed, this cannot be ruled out, but regional structural trends do not appear to be a dominant control on volcano shapes and locations in the region, and limited data show that structure beneath the volcano is oblique to the NE vent alignment trend. Third, variability in S_H directions could be indicative of low-magnitude far field stresses or low-magnitude differences in the horizontal stresses, which would allow local stress sources or perturbations to dominate the stress field (e.g., Heidbach et al., 2007). The prevalence and homogeneous orientation of drilling-induced fractures in core and borehole walls at the Cape Roberts site indicate instead, however, that there are high horizontal stresses and a high horizontal differential stress in the intraplate stress field there (Moos et al., 2000; Wilson and Paulsen, 2000; Jarrard et al., 2001; Wilson and Paulsen, 2001). Fourth, the Morning region may mark a distinct stress province within the rift system. This possibility is supported by the fact that there is a major along-axis offset and trend change of the rift border in the vicinity of Mount Morning (Wilson, 1999; Fitzgerald, 2002); however, new stress data in the Antarctic interior are required to test this hypothesis. Finally, a systematic parallelism between S_H and the rift border may be due to a reorientation of stress along the fundamental lithospheric boundary marked by the Transantarctic Mountains Front fault zone. The boundary along the Transantarctic Mountains rift flank forms the divide between cratonic East Antarctica and the rifted crust of West Antarctica. Seismic data

show that there is a profound change in crustal thickness, mantle velocities, and thermal character across this boundary in the western Ross Sea region (Bannister et al., 2000; Lawrence et al., 2006; Watson et al., 2006). It therefore seems plausible that buoyancy forces associated with this lithospheric discontinuity dominate the intraplate stress regime in this region of the Antarctic plate or, alternatively, that the lithospheric boundary is weak and serves to reorient the stress field (e.g., Mount and Suppe, 1992).

Neotectonic faults reach the seafloor in the western Ross Sea, defining the Terror Rift, a Cenozoic structure superimposed on the Victoria Land rift basin (Cooper et al., 1987; Davey and Brancolini, 1995; Salvini et al., 1997). Previous authors have questioned whether there is active extension across the West Antarctic Rift system (e.g., Finn et al., 2005; Donnellan and Luyendyk, 2004), and the rift system appears to be curiously aseismic (Johnston, 1987). However, extensive faulting at least as young as Pliocene-Pleistocene age has recently been documented in the western portion of the Ross Sea sector of the rift system from marine seismic data (Hall et al., 2007; Henrys et al., 2007), and normal faults cut strata of Pleistocene age cored by the ANDRILL project south of Ross Island (Wilson et al., 2007). Stratigraphic throws imaged in seismic profiles within the Terror Rift are dominated by normal displacement (Cooper et al., 1987; Hall et al., 2007; Henrys et al., 2007), suggesting a normal faulting stress regime with the vertical stress (S_V) > $S_{H'}$. Drilling-induced fractures and borehole studies of the Cape Roberts project indicate a normal faulting (S_V > S_H) to strike-slip faulting (S_H > S_V > S_b) stress regime (Moos et al., 2000; Wilson and Paulsen, 2000; Jarrard et al., 2001; Wilson and Paulsen, 2001). The new stress datum presented herein, together with the S_H directions documented by the Cape Roberts Project and indicated by elongate calderas, is oriented parallel to the Terror Rift fault trends, consistent with Pleistocene and, possibly, active horizontal extension. A contemporary normal to strike-slip fault stress regime is thus indicated for the western Ross Sea sector of the West Antarctic Rift.

Intraplate regions elsewhere in the world are typified by relatively uniform stress fields in which the S_H direction shows little variation over large areas (Zoback et al., 1989; Zoback, 1992). Zoback (1992) interpreted the uniform stress field in intraplate regions to be related to plate-driving mechanisms like the ridge-push force. The Antarctic plate is almost completely surrounded by mid-ocean ridges, much like the African plate, and would be expected to have a compressive intraplate stress regime due to ridge-push forces. Yet, like the East African Rift

in the African continent, the Antarctic continent contains the Cenozoic West Antarctic Rift system (LeMasurier, 1990; Tessensohn and Wörner, 1991). The midplate region of Africa is characterized by a regional compressive stress regime related to the ridge-push force, except in the area of the East African Rift, which is characterized by an extensional stress regime. The East African Rift system, and the world's other active rift systems, are generally characterized by lithospheric thinning and high topography, suggesting that extension in these areas is related to buoyancy forces that dominate the regional compressive stress field generated by the plate-boundary forces (Zoback, 1992). Plate-boundary forces have been suggested to play roles in deformation in rifts, such as the Rio Grande Rift and the East African Rift, where rotation in the orientation of the crustal stress field during rifting has been linked to Pacific–North American plate interactions and ridge-push, respectively (Golembek et al., 1983; Bosworth et al., 1992). Modeling by Steinberger et al. (2001) of lithospheric stresses caused by mantle flow predicts tensional stresses in the Ross Sea region, consistent with Cenozoic extensional intraplate deformation. There is as yet insufficient stress data across the Antarctic plate to define contemporary platewide stress patterns or any changes in stress regime across the plate. In order to determine whether the extensional stress regime in the Ross Sea region results from tractions due to mantle flow, plate-boundary forces, or intraplate buoyancy forces, there is a clear need for continued acquisition of in situ stress data to assess the contemporary geodynamic state of the West Antarctic Rift system.

APPENDIX 1. MAPPING AND RANKING METHODS

We used a combination of existing maps (Wright-Grassham, 1987), SPOT 3 panchromatic satellite imagery (10 m ground resolution), RADARSAT and JERS radar imagery (30 m ground resolution), LANDSAT imagery (Fig. 3; 15–30 m ground resolution), aerial photography (Figs. 8A and 9A), and field work that included helicopter-based digital photography and videography (Figs. 7, 8B, 9B, and 9C). Parasitic vents previously mapped in the area by Wright-Grassham (1987) were included if they could be verified in the field, on aerial photographs or video, or on satellite imagery. We paid particular attention to mapping the linear traces of fissure ridges, the rim shapes of cinder cones, and the outer margins of endogenous domes. In cases where vents lacked shape information, for example, where cinder cones lack definable rims (i.e., cone mounds; Fig. 6C), we mapped the highest point as the vent location. The shapes and locations of coalescing cones were mapped and counted separately. The certainty of each mapped vent, as well as the certainty of the shape of the vents, were classified as definite, probable, possible, and unreliable. The uncertainty in the location and shape of a vent is due to the limit of spatial resolution of the imagery

we used for mapping, the masking of shapes due to the high contrast between the black volcanic cone outcrops and surrounding snow and ice on the imagery, snow and ice cover of cones, and the modification of cone rims due to breaching. Vent compositions were assigned based on previous petrologic interpretations (Wright-Grassham, 1987) and, in some cases, based on our field work and image or photo interpretation.

We systematically distinguished elongate vents from circular vents by constructing best-fit ellipses to match the mapped shape of each cinder cone and dome using a software program written for Arcview® to draw ellipses based on knowledge of the vent center and points along the rim. In cases where cinder cone rims were incomplete (where they are obscured by snow or have been breached, for example, by lava flows), we used the remaining rim to construct the best-fit ellipse. We classified cones with axial ratios (i.e., long axis/short axis) <1.2 as circular, ≥ 1.2 and ≤ 1.8 as elongate, and ≥ 1.8 as cleft cones.

Figure 6C illustrates the use of vent spacing and shapes to identify alignments that mark the subsurface trace of feeder dikes. Vents that are closely spaced or coalesce indicate the presence of an underlying feeder dike. The definition of vent alignments is strongly reinforced when vents are elongate. In these cases, vent alignments are defined by drawing a line through the long axes of elongate vents to other elongate or circular vents along the extension of the same trend. A line connecting several elongate cones of the same trend is most clear. In cases where there is a choice of two possible alignment trends, elongate cones are used to guide the choice, which helps by decreasing the ambiguity in selecting alignments. For example, the cleft and elongate cones between letters A to C, D to F, and G to H in Figure 6C have long axes that trend toward other vents, suggesting that they collectively mark alignments formed by spaced eruptions along subsurface feeder dikes. In contrast, the elongate shapes of cleft and elongate cones do not support the apparent alignments from B to D and C to G. Figures 7, 8, and 9 show examples of aligned elongate and cleft cones used in the identification of alignments on Mount Morning.

Our assessments of alignment rank are based on the following characteristics: (1) the numbers of vents, (2) the standard deviation of cinder cone center points from a best-fit line, (3) the numbers and/or types of elongate cones (Index of Vent Elongation), (4) the standard deviation of the trend of elongate cone long axes from the best-fit line, and (5) the average of the cone spacing distances. We calculated the orientation and best-fit line standard deviation for each alignment by conducting a Deming regression analysis (i.e., orthogonal linear regression), which minimizes the orthogonal distances of vent centers (determined from the best-fit ellipses) to a best-fit line (Deming, 1943). We then calculated the standard deviation of the angular deviation of the long axes of elongate vents from the best-fit line; if there was only one elongate vent, this was taken to be the angular deviation of the vent's long axis from the azimuth. We used all vents, including those that were ranked as "possible" or "unreliable" for vent certainty or shape certainty, in the total number of cones for each alignment and for calculation of the best-fit line. Only vents with definite and probable rankings for vent and shape certainty were considered in the shape criteria for quality ranking. Vent alignments that lacked fissure ridges, cleft cones, or elongate cones were required to have better best-fit line standard deviations and closer average cone spacing in order to be ranked equally with alignments that contained vent shape information.

All but six alignments were ranked using the vent shape ranking criteria. Each alignment was examined to identify and possibly exclude any anomalous shape data that unjustifiably downgraded the quality of the alignment. This appeared to be the case with alignment B6, which had one elongate cone with an anomalous long-axis trend with respect to the azimuth of the alignment and the long axes of other elongate cones within the alignment. This caused a relatively high standard deviation for cone long axes and, thus, a C quality rank for alignment B6. We upgraded alignment B6 to a quality rank of B because the alignment would receive a higher-quality ranking of B if the anomalous cone were excluded.

ACKNOWLEDGMENTS

This work was funded by National Science Foundation (NSF) grant OPP-990970 to T. Wilson and NSF grant OPP-9910879 to T. Paulsen. We thank Yaron Felus and Jon Koenig for support in the field and laboratory aspects of this research, Rick Allmendinger for providing his stereonet program, Yaron Felus who wrote the best-fit ellipse program for Arcview®, William McIntosh and Richard Esser for the argon analyses, and Peter Braddock for his assistance in the field. We also thank John Foden, Richard Price, Manfred Strecker, Julie Rowland, and an anonymous reviewer for helpful critiques that improved this manuscript. Paulsen acknowledges the University of Wisconsin Faculty Sabbatical Program for release time to work on this project.

REFERENCES CITED

- Adiyaman, O., Chorowicz, J., and Kose, O., 1998, Relationships between volcanic patterns and neotectonics in Eastern Anatolia from analysis of satellite images and DEM: *Journal of Volcanology and Geothermal Research*, v. 85, p. 17–32, doi: 10.1016/S0377-0273(98)00047-X.
- Anderson, E.M., 1951, *The Dynamics of Faulting and Dyke Formation with Application to Britain*: Edinburgh, Oliver and Boyd, Ltd., 206 p.
- Armstrong, R.L., 1978, K-Ar dating: Late Cenozoic McMurdo Volcanic Group and Dry Valley glacial history, Victoria Land, Antarctica: *New Zealand Journal of Geology and Geophysics*, v. 21, p. 685–698.
- Bannister, S., Snieder, R.K., and Passier, M.L., 2000, Shear-wave velocities under the Transantarctic Mountains and Terror Rift from surface wave inversion: *Geophysical Research Letters*, v. 27, p. 281–284, doi: 10.1029/1999GL010866.
- Behrendt, J.C., LeMasurier, W.E., Cooper, A.K., Tessensohn, F., Tréhu, A., and Damaske, D., 1991, Geophysical studies of the West Antarctic Rift system: *Tectonics*, v. 10, p. 1257–1273, doi: 10.1029/91TC00868.
- Behrendt, J.C., Saltus, R., Damaske, D., McCafferty, A., Finn, C.A., Blankschap, D., and Bell, R.E., 1996, Patterns of late Cenozoic volcanic and tectonic activity in the West Antarctic Rift system revealed by aeromagnetic surveys: *Tectonics*, v. 15, p. 660–676, doi: 10.1029/95TC03500.
- Bosum, W., Damaske, N.W., Rolan, N.W., Behrendt, J.C., and Saltus, R.W., 1989, The GANOVEX IV Victoria Land/Ross Sea aeromagnetic survey: Interpretation of anomalies: *Geologisches Jahrbuch Reihe E*, v. 38, p. 153–230.
- Bosworth, W., and Strecker, M.R., 1997, Stress field changes in the Afro-Arabian Rift system during the Miocene to Recent period: *Tectonophysics*, v. 278, p. 47–62, doi: 10.1016/S0040-1951(97)00094-2.
- Bosworth, W., Strecker, M.R., and Blisniuk, P.M., 1992, Integration of East African paleostress and present-day stress data: Implications for continental stress field dynamics: *Journal of Geophysical Research*, v. 97, p. 11,851–11,865, doi: 10.1029/90JB02568.
- Bosworth, W., Burke, K., and Strecker, M., 2000, Magma chamber elongation as an indicator of intraplate stress field orientation: Borehole breakout mechanism and examples from the late Pleistocene to Recent Kenya

TABLE A1. QUALITY RANKING FOR CONE ALIGNMENTS

Quality Rank	# Vents	Standard Deviation Best Fit Line Distance (m)	Index of Vent Elongation	Standard Angular Deviation Vent Long Axes (°)	Average Vent Spacing Distance (m)
A	≥4	≤125	1 Cleft Cone -or- 1 Fissure Ridge -or- 2 ≥1.6 -or- 1 ≥1.6 and 1 ≥1.4	≤30	No Limit
	≥5	≤100	No Shape Data	No Shape Data	≤600
B	≥3	≤150	1 ≥1.6 -or- 2 ≥1.4 -or- 1 ≥1.5 and 2 ≥1.2	≤35	No Limit
	≥4	≤125	No Shape Data	No Shape Data	≤600
C	≥2	≤175	1 ≥1.4 -or- 2 ≥1.2	≤40	No Limit
	≥3	≤150	No Shape Data	No Shape Data	≤800
D	≥2	>175	1 ≥1.2	>45	No Limit
	≥3	>150	No Shape Data	No Shape Data	>800

Notes: The A quality thresholds for the standard deviation of best fit line distance and standard angular deviation vent long axes are based on our measurements of cone alignments along fissures in Iceland (Thordarson, 1993), Hawaii (Wolfe and Morris, 1996), the Makushin stratovolcano (Drewes et al., 1961), and Lunar Craters (Scott and Trask, 1971). The lower reliability thresholds that define rankings B, C, and D are defined as progressively lower steps from the thresholds that define A-ranked alignments. The thresholds for the average vent spacing distance are based on our measurements of cone alignments along fissures in Hawaii and on the Makushin stratovolcano, as well as on the modal average vent spacing distances for parasitic cones on the flanks of polygenetic volcanoes, which typically range from 600 m and 800 m (Settle, 1979).

TABLE A2. VOLCANIC ALIGNMENTS ON MOUNT MORNING AND MASON SPUR, MCMURDO SOUND, ANTARCTICA

Alignment Rank/ID#	Location (°)	Rock Type	Latitude (°S)	Longitude (°E)	Length (km)	# Vents	FR, CC, and EV Axial Ratios	Standard Deviation Best Fit Line Distance (m)	Standard Angular Deviation Vent Long Axes (°)	Average Vent Spacing Distance (m)	Alignment Azimuth (°)
A1	HR	P/B	-78.49	163.88	6.5	11	2 CC, 1.3	101	25	1118	37
A2	HR	B	-78.45	164.19	8.4	11	3 CC, 1.5, 1.4, 1.3	105	5	857	47
A3	HR	B	-78.40	164.24	2.7	9	2 CC, 1.3, 1.3	61	3	322	58
A4	HR	B	-78.39	164.20	5.1	5	CC, 1.7, 1.6, 1.4	66	20	833	47
A5	HR	B	-78.38	164.23	0.6	6	FR, 1.2	10	28	122	341
B1	RR	P	-78.48	163.57	2.6	3	CC	56	2	874	17
B2	RR	P/B	-78.44	163.44	0.6	4	NA	10	NA	201	24
B3	RR	B	-78.44	163.54	0.9	3	CC, 1.7 ^a	110	13 ^b , 4 ^c	484	26
B4	RR	P/B	-78.44	163.73	5.6	6	CC, 1.5 ^a , 1.5 ^a , 1.4 ^a	107	5 ^b , 9 ^c	1114	24
B5	RR	T	-78.37	163.79	0.5	3	NA	7	NA	269	67
B6	HR	B	-78.41	164.09	10.6	6	1.7, 1.5, 1.3	52	37	2107	17
B7	HR	B	-78.43	164.18	2.8	4	CC ^a	56	9 ^c	365	34
B8	HR	B	-78.41	164.46	4.7	6	CC, 1.3, 1.2	127	29	1263	7
B9	MS	B	-78.54	164.35	2	3	CC	40	2	1032	56
C1	HR	B	-78.38	164.07	3.8	5	CC ^a , 1.4, 1.2	34	6 ^b , 6 ^c	1333	34
C2	HR	B	-78.43	164.16	3.7	4	FR ^a , 1.5	21	8	1233	33
D1	RR	P	-78.45	163.38	2.4	3	NA	33	NA	1269	23
D2	RR	P	-78.48	163.44	3.1	3	NA	80	NA	1570	4
D3	RR	B	-78.40	163.83	7.8	4	1.7	190	33	2609	28
D4	MS	B	-78.55	164.38	2.5	3	NA	13	NA	1279	35
D5	RR	B	-78.36	163.72	2.5	4	1.3	168	12	839	25
D6	HR	B	-78.48	163.88	7.1	5	1.3	115	5	1774	46
D7	RR	B	-78.37	163.74	3.5	3	FR ^a , CC ^a	14	15 ^c	1849	305

Note: HR—Hurricane Ridge; RR—Riviera Ridge; B—Basalt; P—Phonolite; T—Trachyte; E—Elongate; CC—Cleft Cone; FR—Fissure Ridge; EV—Elongate Vent; NA—Not Applicable.

^aFissure ridge, cleft cone, or elongate vent not included because of possible or unreliable vent or shape certainty ranking.

^bStandard deviation vent long axes calculated without vents of possible or unreliable vent or shape certainty ranking.

^cStandard deviation vent long axes calculated with vents of possible or unreliable vent or shape certainty ranking.

- Rift Valley, in Jessell, M.W., and Urai, J.L., eds., Stress, Strain, and Structure: A Volume in Honor of W.D. Means: Journal of the Virtual Explorer, v. 2, <http://virtualexplorer.com.au/special/meansvolume/contribs/bosworth/index.html>.
- Bosworth, W., Burke, K., and Strecker, M., 2003, Effects of stress fields on magma chamber stability and the formation of collapse calderas: Tectonics, v. 22, p. 1042, doi: 10.1029/2002TC001369.
- Bott, M.H.P., and Stern, T.A., 1992, Finite element analysis of Transantarctic Mountain uplift and coeval subsidence in the Ross embayment: Tectonophysics, v. 201, p. 341–356, doi: 10.1016/0040-1951(92)90241-W.
- Breed, W.J., 1964, Morphology and lineation of cinder cones in the San Franciscan volcanic field: Museum of Northern Arizona Bulletin, v. 40, p. 65–71.
- Chadwick, W.W., Jr., and Dieterich, J.H., 1995, Mechanical modeling of circumferential and radial dike intrusion on Galapagos volcanoes: Journal of Volcanology and Geothermal Research, v. 66, p. 37–52, doi: 10.1016/0377-0273(94)00060-T.
- Chadwick, W.W., Jr., and Howard, K.A., 1991, The pattern of circumferential and radial eruptive fissures on the volcanoes Fernandina and Isabela Islands, Galapagos: Bulletin of Volcanology, v. 53, p. 259–275, doi: 10.1007/BF00414523.
- Chevallier, L., and Verwoerd, W.J., 1988, A numerical model for the mechanical behavior of intraplate volcanoes: Journal of Geophysical Research, v. 93, p. 4182–4198, doi: 10.1029/JB093iB05p04182.
- Chiappini, M., Ferraccioli, F., Bozzo, E., and Damaske, D., 2002, Regional compilation and analysis of aeromagnetic anomalies for the Transantarctic Mountains–Ross Sea sector of the Antarctic: Tectonophysics, v. 347, p. 121–137, doi: 10.1016/S0040-1951(01)00241-4.
- Chorowicz, J., Bardintzeff, J.M., Rasamimanana, G., Chotin, P., Thouin, C., and Rudant, J.P., 1997, An approach using SAR ERS images to relate extension fractures to volcanic vents: Examples from Iceland and Madagascar: Tectonophysics, v. 271, p. 263–283, doi: 10.1016/S0040-1951(96)00250-8.
- Coblentz, D.D., Fitzgerald, P.G., Richardson, R.M., and Sandiford, M., 1995, The Antarctic intraplate stress field: Cretaceous to Present: Eos (Transactions, American Geophysical Union), v. 76, no. 46, p. 577.
- Cook, Y.A., and Craw, D., 2001, Amalgamation of disparate crustal fragments in the Walcott Bay–Foster Glacier area, South Victoria Land, Antarctica: New Zealand Journal of Geology and Geophysics, v. 44, p. 403–416.
- Cooper, A.K., Davey, F.J., and Behrendt, J.C., 1987, Seismic stratigraphy and structure of the Victoria Land basin, western Ross Sea, Antarctica, in Cooper, A.J., and Davey, F.J., eds., The Antarctic Continental Margin: Geology and Geophysics of the Western Ross Sea: Houston, Texas, Circum-Pacific Council for Energy and Mineral Resources, p. 27–76.
- Damaske, D., Behrendt, J.C., McCafferty, A.E., Saltus, R.W., and Meyer, U., 1994, Transfer faults in the west Ross Sea: New evidence from the McMurdo Sound/Ross Ice Shelf aeromagnetic survey (GANOVEX VI): Antarctic Science, v. 6, p. 359–364, doi: 10.1017/S0954102094000556.
- Davey, F.J., and Brancolini, G., 1995, The late Mesozoic and Cenozoic structural setting of the Ross Sea region, in Cooper, A.J., et al., eds., Geology and Seismic Stratigraphy of the Antarctic Margin: Washington, D.C., American Geophysical Union, Antarctic Research Series, v. 68, p. 167–182.
- Delaney, P.T., and Pollard, D.D., 1982, Solidification of basaltic magma during flow in a dike: American Journal of Science, v. 282, p. 856–885.
- Delaney, P.T., Pollard, D.D., Ziony, J.I., and McKee, E.H., 1986, Field relations between dikes and joints: Emplacement processes and paleostress analysis: Journal of Geophysical Research, v. 91, p. 4920–4938, doi: 10.1029/JB091iB05p04920.
- Deming, W.E., 1943, Statistical Adjustment of Data: New York, John Wiley & Sons. Reprinted: 1964, New York, Dover Publications, Inc., 184 p.
- Donnellan, A., and Luyendyk, B.P., 2004, GPS evidence for a coherent Antarctic plate and for post-glacial rebound in Marie Byrd Land: Global and Planetary Change, v. 42, p. 305–311, doi: 10.1016/j.gloplacha.2004.02.006.
- Drewes, H., Fraser, G.D., Snyder, G.L., and Barnet, H.F., 1961, Geology of the Unalaska Island and adjacent insular shelf, Aleutian Islands, Alaska: United States Geological Survey Bulletin 1028-S, p. 583–676.
- Findlay, R.H., Craw, D., and Skinner, D.N.B., 1984, Lithostratigraphy and structure of the Koettlitz Group, McMurdo Sound, Antarctica: New Zealand Journal of Geology and Geophysics, v. 27, p. 513–536.
- Finn, C.A., Muller, R.D., and Panter, K.S., 2005, A Cenozoic diffuse alkaline magmatic province (DAMP) in the southwest Pacific without rift or plume origin: Geochemistry, Geophysics, Geosystems, v. 6, doi: 10.1029/2004GC000723.
- Fitzgerald, P.G., 1992, The Transantarctic Mountains of southern Victoria Land: The application of apatite fission track analysis to a rift shoulder uplift: Tectonics, v. 11, p. 634–662, doi: 10.1029/91TC02495.
- Fitzgerald, P.G., 2002, Tectonics and landscape evolution of the Antarctic plate since the breakup of Gondwana, with an emphasis on the West Antarctic Rift system and the Transantarctic Mountains, in Henrys, S., et al., eds., Antarctica at the Close of a Millennium: Royal Society of New Zealand Bulletin, v. 35, p. 453–469.
- Franz, G., Breitkreuz, C., Coyle, D.A., El Hu, B., Heinrich, W., Paulick, H., Pudlo, D., Smith, R., and Steiner, G., 1997, The alkaline Meidob volcanic field (late Cenozoic, northwest Sudan): Journal of African Earth Sciences, v. 25, p. 263–291, doi: 10.1016/S0899-5362(97)00103-6.
- Golombek, M.P., McGill, G.E., and Brown, L., 1983, Tectonic and geologic evolution of the Espanola Basin, Rio Grande Rift: Structure, rate of extension, and relation to the state of stress in the western United States: Tectonophysics, v. 94, p. 483–507, doi: 10.1016/0040-1951(83)90031-8.
- Gradstein, F.M., Ogg, J.G., Smith, A.G., Agterberg, F.P., Bleeker, W., Cooper, R.A., Davydov, V., Gibbard, P., Hinnov, L.A., House, M.R., Lourens, L., Luterbacher, H.P., McArthur, J., Melchin, M.J., Robb, L.J., Shergold, J., Villeneuve, M., Wardlaw, B.R., Ali, J., Brinkhuis, H., Hilgen, F.J., Hooker, J., Howarth, R.J., Knoll, A.H., Laskar, J., Monechi, S., Plumb, K.A., Powell, J., Raffi, I., Röhl, U., Sadler, P., Sanfilippo, A., Schmitz, B., Shackleton, N.J., Shields, G.A., Strauss, H., Van Dam, J., van Kolfschoten, T., Veizer, J., and Wilson, D., 2004, A Geological Time Scale 2004: Cambridge, Cambridge University Press, 589 p.
- Haimson, B.C., 1975, Deep in-situ stress measurements by hydro fracturing: Tectonophysics, v. 29, p. 41–47, doi: 10.1016/0040-1951(75)90131-6.
- Hall, J.M., Wilson, T.J., and Henrys, S.A., 2007, Structure of central Terror Rift, western Ross Sea, Antarctica, in Cooper, A.K., et al., eds., Antarctica: A Keystone in a Changing World: Online Proceedings of the 10th International Symposium on Antarctic Earth Sciences: U.S. Geological Survey Open-File Report 2007–1047, Short Research Paper 108; doi: 10.3133/of2007-1047.srp108.
- Haran, T., Bohlander, J., Scambos, T., and Fahnestock, M., compilers, 2005, MODIS Mosaic of Antarctica (MOA) Image Map: Boulder, Colorado, National Snow and Ice Data Center: Digital media.
- Haug, G.H., and Strecker, M.R., 1995, Volcano-tectonic evolution of the Chyulu Hills and implications for the regional stress field in Kenya: Geology, v. 23, no. 2, p. 165–168, doi: 10.1130/0091-7613(1995)023<0165:VTEOTC>2.3.CO;2.
- Heidbach, O., Reinecker, J., Tingay, M., Müller, B., Sperner, B., Fuchs, K., and Wenzel, F., 2007, Plate boundary forces are not enough: Second- and third-order stress patterns highlighted in the World Stress Map database: Tectonics, v. 26, p. TC6014, doi: 10.1029/2007TC002133.
- Heidbach, O., Tingay, M., Barth, A., Reinecker, J., Kurfeß, D., Müller, B., 2008, The 2008 release of the World Stress Map, <http://www.world-stress-map.org>.
- Henrys, S.A., Wilson, T.J., Whittaker, J.M., Fielding, C., Hall, J.M., and Naish, T., 2007, Tectonic history of mid-Miocene to present southern Victoria Land Basin, inferred from seismic stratigraphy in McMurdo Sound, Antarctica, in Cooper, A.K., et al., eds., Antarctica: A Keystone in a Changing World: Online Proceedings of the 10th International Symposium on Antarctic Earth Sciences: U.S. Geological Survey Open-File Report
- 2007–1047, Short Research Paper 049, doi: 10.3133/of2007-1047.srp049.
- Holohan, E.P., Troll, V.R., Walter, T.R., Munn, S., McDonnell, S., and Shipton, Z.K., 2005, Elliptical calderas in active tectonic settings: An experimental approach: Journal of Volcanology and Geothermal Research, v. 144, p. 119–136, doi: 10.1016/j.jvolgeores.2004.11.020.
- Illies, J.H., and Greiner, G., 1978, Rhine graben and the Alpine system: Geological Society of America Bulletin, v. 89, p. 770–782, doi: 10.1130/0016-7606(1978)89<770:RATAS>2.0.CO;2.
- Illies, J.H., Baumann, H., and Hoffmann, B., 1981, Stress pattern and strain release in the Alpine foreland: Tectonophysics, v. 71, p. 157–172, doi: 10.1016/0040-1951(81)90059-7.
- Ivins, E.R., James, T.S., and Kleemann, V., 2003, Glacial isostatic stress shadowing by the Antarctic Ice Sheet: Journal of Geophysical Research, v. 108, p. 2560, doi: 10.1029/2002JB002182.
- Jarrard, R.D., Moos, D., Wilson, T., Bücker, C.B., and Paulsen, T., 2001, Stress patterns observed by borehole televIEWER logging of the CRP-3 drillhole, Victoria Land Basin, Antarctica: Terra Antarctica, v. 8, p. 197–204.
- Johnston, A.C., 1987, Suppression of earthquakes by large continental ice sheets: Nature, v. 330, p. 467–469, doi: 10.1038/330467a0.
- Jones, S., 1997, Late Quaternary faulting and neotectonics, south Victoria Land, Antarctica: Journal of the Geological Society of London, v. 154, p. 645–652, doi: 10.1144/gsjgs.154.4.0645.
- Korme, T., Chorowicz, B., Collet, B., and Bonavia, F.F., 1997, Volcanic vents rooted on extension fractures and their geodynamic implications in the Ethiopian Rift: Journal of Volcanology and Geothermal Research, v. 79, p. 205–222, doi: 10.1016/S0377-0273(97)00034-6.
- Kurz, M.D., and Ackert, R.P., 1996, History of the West Antarctic Ice Sheet: Some new evidence from southern McMurdo Sound: Third Annual West Antarctic Ice Sheet Initiative Workshop: Algonkian, Virginia, 25–27 September 1996, <http://neptune.gsfc.nasa.gov/wais/pastmeetings/abstracts96/kurz.html>.
- Kyle, P.R., 1990a, McMurdo Volcanic Group, western Ross Embayment: Introduction, in LeMasurier, W.E., and Thomson, J.W., eds., Volcanoes of the Antarctic Plate and Southern Ocean: Washington, D.C., American Geophysical Union, Antarctic Research Series, v. 48, p. 19–25.
- Kyle, P.R., 1990b, Erebus Volcanic Province, in LeMasurier, W.E., and Thomson, J.W., eds., Volcanoes of the Antarctic Plate and Southern Ocean: Washington, D.C., American Geophysical Union, Antarctic Research Series, v. 48, p. 81–88.
- Kyle, P.R., and Cole, J.W., 1974, Structural control of volcanism in the McMurdo Volcanic Group, Antarctica: Bulletin of Volcanology, v. 38, p. 16–25, doi: 10.1007/BF02597798.
- Kyle, P.R., and Muney, H.L., 1989, Geology and geochronology of McMurdo Volcanic Group rocks in the vicinity of Lake Morning, McMurdo Sound, Antarctica: Antarctic Science, v. 1, p. 345–350, doi: 10.1017/S0954102089000520.
- Lawrence, J.F., Wiens, D.A., Nyblade, A.A., Anandakrishnan, S., Shore, P.J., and Voigt, D., 2006, Rayleigh wave phase velocity analysis of the Ross Sea, Transantarctic Mountains, and East Antarctica from a temporary seismograph array: Journal of Geophysical Research, v. 111, doi: 10.1029/2005JB003812.
- LeMasurier, W.E., 1990, Late Cenozoic volcanism on the Antarctic plate—An overview, in LeMasurier, W.E., and Thomson, J.W., eds., Volcanoes of the Antarctic Plate and Southern Ocean: Washington, D.C., American Geophysical Union, Antarctic Research Series, v. 48, p. 1–19.
- Lithgow-Bertelloni, C., and Guynn, J.H., 2004, Origin of the lithospheric stress field: Journal of Geophysical Research, v. 109, p. B01408, doi: 10.1029/2003JB002467.
- MacDonald, G.A., 1972, Volcanoes: Englewood Cliffs, New Jersey, Prentice Hall, Inc., 510 p.
- McIntosh, W.C., and Esser, R., 2005, ^{40}Ar – ^{39}Ar Geochronology Results from McMurdo Sound Area, Antarctica: New Mexico Bureau of Geology and Mineral Resources Open-File Report, OF-AR-34, 50 p.
- McIntosh, W.C., and Kyle, P.R., 1990, A.I. Hallet Volcanic Province—Summary, in LeMasurier, W.E., and Thomson, J.W., eds., Volcanoes of the Antarctic Plate and

- Southern Ocean: Washington, D.C., American Geophysical Union, Antarctic Research Series, v. 48, p. 26–31.
- Moos, D., Jarrard, R., Paulsen, T., Scholz, E., and Wilson, T., 2000, Acoustic borehole televIEWer (BHTV) results from the CRP2A core hole: *Terra Antarctica*, v. 7, p. 279–286.
- Mortimer, E., Paton, D.A., Scholz, C.A., Strecker, M.R., and Blisniuk, P., 2007, Orthogonal to oblique rifting: Effect of rift basin orientation in the evolution of the North basin, Malawi Rift, East Africa: *Basin Research*, v. 19, p. 393–407, doi: 10.1111/j.1365-2117.2007.00332.x.
- Mount, V.S., and Suppe, J., 1992, Present-day stress orientation adjacent to active strike-slip faults: California and Sumatra: *Journal of Geophysical Research*, v. 97, p. 11,995–12,013, doi: 10.1029/92JB00130.
- Muller, O.H., and Pollard, D.D., 1977, The stress state near Spanish Peaks, Colorado, determined from a dike pattern: *Pure and Applied Geophysics*, v. 115, p. 69–86, doi: 10.1007/BF01637098.
- Muncy, H.L., 1979, Geologic History and Petrogenesis of Alkaline Volcanic Rocks, Mount Morning, Antarctica [M.Sc. thesis]: Columbus, The Ohio State University, 112 p.
- Nakamura, K., 1977, Volcanoes as possible indicators of tectonic stress orientation—Principal and proposal: *Journal of Volcanology and Geothermal Research*, v. 2, p. 1–16, doi: 10.1016/0377-0273(77)90012-9.
- Nakamura, K., Jacob, K.H., and Davies, J.N., 1977, Volcanoes as possible indicators of tectonic stress orientation—Aleutians and Alaska: *Pure and Applied Geophysics*, v. 115, p. 87–112, doi: 10.1007/BF01637099.
- Odé, H., 1957, Mechanical analysis of the dike pattern of the Spanish Peaks area, Colorado: *Geological Society of America Bulletin*, v. 68, p. 567–576, doi: 10.1130/0016-7606(1957)68[567:MAOTDP]2.0.CO;2.
- Parsons, T., and Thompson, G.A., 1991, The role of magma overpressure in suppressing earthquakes and topography: Worldwide examples: *Science*, v. 253, p. 1399–1402, doi: 10.1126/science.253.5026.1399.
- Paulsen, T.S., and Wilson, T.J., 2007, Elongate summit calderas as Neogene paleostress indicators in Antarctica, in Cooper, A.K., et al., eds., *Antarctica: A Keystone in a Changing World: Online Proceedings of the 10th International Symposium on Antarctic Earth Sciences: U.S. Geological Survey Open-File Report 2007-1047, Short Research Paper 072*, doi: 10.3133/of2007-1047.srp072.
- Polyakov, M.M., Krylov, A., and Mazina, T.I., 1976, New data on radiogeochronology of Antarctic Cenozoic vulcanites 160°E–100°W: *Information Bulletin of the Soviet Antarctica Expedition*, v. 93, p. 19–26 (in Russian).
- Reading, A., 2002, Antarctic seismicity and neotectonics, in Henrys, S., et al., eds., *Antarctica at the Close of a Millennium: Royal Society of New Zealand Bulletin*, v. 35, p. 479–484.
- Reading, A.M., 2006, On seismic strain-release within the Antarctic plate, in Damaske, D., et al., eds., *Antarctica, Contributions to Global Earth Sciences*: Berlin-Heidelberg, Springer-Verlag, v. 9, p. 351–356.
- Renne, P.R., Swisher, C.C., Deino, A.L., Karner, D.B., Owens, T.L., and Depaolo, D.J., 1998, Intercalibration of standards: Absolute ages and uncertainties in ^{40}Ar - ^{39}Ar dating: *Chemical Geology*, v. 145, p. 117–152, doi: 10.1016/S0009-2541(97)00159-9.
- Ring, U., Betzler, C., and Delvaux, D., 1992, Normal vs. strike-slip faulting during rift development in East Africa: The Malawi Rift: *Geology*, v. 20, p. 1015–1018, doi: 10.1130/0091-7613(1992)020<1015:NVSFD>2.3.CO;2.
- Rocchi, S., Armienti, P., D'Orazio, M., Tonarini, S., Wijbrans, J., and Di Vincenzo, G., 2002, Cenozoic magmatism in the western Ross Embayment: Role of mantle plume vs. plate dynamics in the development of the West Antarctic Rift system: *Journal of Geophysical Research*, v. 107, p. 2195, doi: 10.1029/2001JB000515.
- Rocchi, S., Storti, F., Di Vincenzo, G., and Rossetti, F., 2003, Intraplate strike-slip tectonics as alternative to mantle plume activity for the Cenozoic rift magmatism in the Ross Sea region, Antarctica, in Storti, F., et al., eds., *Intraplate Strike-Slip Deformation Belts: Geological Society of London Special Publication* 210, p. 158–171.
- Rossetti, F., Storti, F., and Salvini, F., 2000, Cenozoic noncoaxial transtension along the western shoulder of the Ross Sea, Antarctica, and the emplacement of McMurdo dyke arrays: *Terra Nova*, v. 12, p. 60–66, doi: 10.1046/j.1365-3121.2000.00270.x.
- Salvini, F., Brancolini, G., Busetti, M., Storti, F., Mazzarini, F., and Coren, F., 1997, Cenozoic geodynamics of the Ross Sea region, Antarctica: *Journal of Geophysical Research*, v. 102, p. 24,669–24,696, doi: 10.1029/97JB01643.
- Scott, D.H., and Trask, N.J., 1971, Geology of the Lunar Crater volcanic field, Nye County, Nevada: U.S. Geological Survey Professional Paper 599-I, p. 1–22.
- Settle, M., 1979, The structure and emplacement of cinder cone fields: *American Journal of Science*, v. 279, p. 1089–1107.
- Simkin, T., 1972, Origin of some flat-topped volcanoes and guyots, in Shagam, R., Hargraves, R.B., Morgan, W.J., Van Houton, F.B., Burk, C.A., Holland, H.D., and Hollister, L.C., eds., *Studies in Earth and Space Sciences: Geological Society of America Memoir* 132, p. 183–193.
- Sperner, B., Müller, B., Heidbach, O., Delvaux, D., Reinicker, J., and Fuchs, K., 2003, Tectonic stress in the Earth's crust: Advances in the World Stress Map project, in Niewland, D.A., ed., *New Insights into Structural Interpretation and Modeling: Geological Society of London Special Publication* 212, p. 101–116.
- Steinberger, B., Marquart, G., and Schmeling, H., 2001, Large-scale lithospheric stress field and topography induced by global mantle circulation: *Earth and Planetary Science Letters*, v. 186, p. 75–91, doi: 10.1016/S0012-821X(01)00229-1.
- Stern, T.A., and ten Brink, U.S., 1989, Flexural uplift of the Transantarctic Mountains: *Journal of Geophysical Research*, v. 94, p. 10,315–10,330, doi: 10.1029/JB094iB08p10315.
- Stewart, I.S., Sauber, J., and Rose, J., 2000, Glacio-seismotectonics; ice sheets, crustal deformation and seismicity: *Quaternary Science Reviews*, v. 19, p. 1367–1389.
- Strecker, M.R., Blisniuk, P.M., and Eibach, G.H., 1990, Rotation of extension direction in the central Kenya Rift: *Geology*, v. 18, p. 299–302, doi: 10.1130/0091-7613(1990)018<0299:ROEDIT>2.3.CO;2.
- Stuiver, M., and Braziunas, T.F., 1985, Compilation of isotopic dates from Antarctica: *Radiocarbon*, v. 27, p. 117–304.
- Suter, M., 1991, State of stress and active deformation in Mexico and western Central America, in Slemmons, D.B., et al., eds., *Neotectonics of North America: Boulder*, Geological Society of America, Geological Society of America Decade Map, v. 1, p. 401–421.
- Suter, M., Quintero, O., and Johnson, C.A., 1992, Active faults and state of stress in the central part of the Trans-Mexican volcanic belt, Mexico: I. The Venta de Bravo fault: *Journal of Geophysical Research*, v. 97, p. 11,983–11,993, doi: 10.1029/91JB00428.
- ten Brink, U.S., Hackney, R.I., Bannister, S., Stern, T.A., and Makovsky, Y., 1997, Uplift of the Transantarctic Mountains and the bedrock beneath the East Antarctic Ice Sheet: *Journal of Geophysical Research*, v. 102, p. 27,603–27,621, doi: 10.1029/97JB02483.
- Tessensohn, F., and Wörner, G., 1991, The Ross Sea rift system, Antarctica: Structure, evolution and analogues, in Thomson, M.R.A., et al., eds., *Geological Evolution of Antarctica*: New York, Cambridge University Press, p. 273–277.
- Thordarson, Th., and Self, S., 1993, The Laki (Skaftárr) Fires and Grímsvötn eruptions in 1783–1785: *Bulletin of Volcanology*, v. 55, p. 233–263, doi: 10.1007/BF00624353.
- Tibaldi, A., 1995, Morphology of pyroclastic cones and tectonics: *Journal of Geophysical Research*, v. 100, p. 24,521–24,535, doi: 10.1029/95JB02250.
- Warren, G., 1969, *Geology of the Terra Nova Bay–McMurdo Sound Area, Victoria Land*: New York, American Geographical Society, Antarctic Map Folio Series, folio 12, plate 13.
- Watson, T., Nyblade, A., Wiens, D., Anandakrishnan, S., Benoit, M., Shore, P., Voigt, D., and VanDecar, J., 2006, P and S velocity structure of the upper mantle beneath the Transantarctic Mountains, East Antarctic craton, and Ross Sea from travel time tomography: *Geochemistry, Geophysics, Geosystems*, v. 7, p. Q07005, doi: 10.1029/2005GC001238.
- Wilson, T.J., 1995, Cenozoic transtension along the Transantarctic Mountains–West Antarctic Rift boundary, southern Victoria Land, Antarctica: *Tectonics*, v. 14, p. 531–545, doi: 10.1029/94TC02441.
- Wilson, T.J., 1999, Cenozoic structural segmentation of the Transantarctic Mountains rift flank in southern Victoria Land, Antarctica, in van der Wateren, F.M., and Cloetingh, S., *Lithosphere Dynamics and Environmental Change of the Cenozoic West Antarctic Rift System: Global and Planetary Change*, v. 23, p. 105–127, doi: 10.1016/S0921-8181(99)00053-3.
- Wilson, T., and Paulsen, T., 2000, Brittle deformation patterns of CRP2/2A, Victoria Land Basin, Antarctica: *Terra Antarctica*, v. 7, p. 287–298.
- Wilson, T., and Paulsen, T., 2001, Fault and fracture patterns in the CRP-3 core, Victoria Land Basin, Antarctica: *Terra Antarctica*, v. 8, p. 177–196.
- Wilson, T., Paulsen, T., Läufer, A., Millan, C., and the ANDRILL-MIS Science Team, 2007, Fracture logging of the AND-1B core, ANDRILL McMurdo Ice Shelf Project, Antarctica: *Terra Antarctica*, v. 14, p. 109–328.
- Wolfe, E.W., and Morris, J., 1996, *Geologic Map of the Island of Hawaii: U.S. Geological Survey Miscellaneous Investigations Series Map I-2524-A*, scale 1:100,000.
- Wright, A.C., and Kyle, P.R., 1990a, Mount Morning, in LeMasurier, W.E., and Thomson, J.W., eds., *Volcanoes of the Antarctic Plate and Southern Ocean: Washington, D.C., American Geophysical Union, Antarctic Research Series*, v. 48, p. 124–127.
- Wright, A.C., and Kyle, P.R., 1990b, Mason Spur, in LeMasurier, W.E., and Thomson, J.W., eds., *Volcanoes of the Antarctic Plate and Southern Ocean: Washington, D.C., American Geophysical Union, Antarctic Research Series*, v. 48, p. 128–130.
- Wright-Grassham, A.C., 1987, *Volcanic Geology, Mineralogy, and Petrogenesis of the Discovery Volcanic Province, Southern Victoria Land, Antarctica* [Ph.D. thesis]: Socorro, New Mexico Tech, 460 p.
- Wu, P., and Johnston, P., 2000, Can deglaciation trigger earthquakes in N. America?: *Geophysical Research Letters*, v. 27, p. 1323–1326, doi: 10.1029/1999GL011070.
- Zoback, M.L., 1992, First- and second-order patterns of stress in the lithosphere: The World Stress Map project: *Journal of Geophysical Research*, v. 97, p. 11,703–11,728, doi: 10.1029/92JB00132.
- Zoback, M.L., Zoback, M.D., Adams, J., Assumpcao, M., Bell, S., Bergman, E.A., Blümling, P., Bereton, N.R., Denham, D., Ding, J., Fuchs, K., Gay, N., Gregerson, S., Gupta, H.K., Gvishiani, A., Jacob, K., Klein, R., Knoll, P., Magee, M., Mercier, J.L., Müller, B.C., Paquin, C., Rajendran, J., Stephansson, O., Suarez, G., Suter, M., Udias, A., Xu, Z.H., and Zhizhin, M., 1989, Global patterns of tectonic stress: *Nature*, v. 341, p. 291–298, doi: 10.1038/341291a0.

MANUSCRIPT RECEIVED 24 SEPTEMBER 2007

REVISED MANUSCRIPT RECEIVED 9 MAY 2008

MANUSCRIPT ACCEPTED 5 JUNE 2008

PRINTED IN THE USA